Atmospheric
Chemistry
and Physics

Disparities in particulate matter (PM$_{10}$) origins and oxidative potential at a city scale (Grenoble, France) – Part 1: Source apportionment at three neighbouring sites

Lucille Joanna S. Borlaza[1], **Samuël Weber**[1], **Gaëlle Uzu**[1], **Véronique Jacob**[1], **Trishalee Cañete**[1], **Steve Micallef**[4], **Cécile Trébuchon**[4], **Rémy Slama**[5], **Olivier Favez**[2,3], and **Jean-Luc Jaffrezo**[1]

[1]University Grenoble Alpes, CNRS, IRD, INP-G, IGE (UMR 5001), 38000 Grenoble, France
[2]INERIS, Parc Technologique Alata, BP 2, 60550 Verneuil-en-Halatte, France
[3]Laboratoire Central de Surveillance de la Qualité de l'Air (LCSQA), 60550 Verneuil-en-Halatte, France
[4]Atmo Auvergne-Rhônes Alpes, 38400 Grenoble, France
[5]IAB, Team of Environmental Epidemiology applied to Reproduction and Respiratory Health,
University of Grenoble Alpes, 38000 Grenoble, France

Correspondence: Lucille Joanna Borlaza (lucille-joanna.borlaza@univ-grenoble-alpes.fr) and
Jean-Luc Jaffrezo (jean-luc.jaffrezo@univ-grenoble-alpes.fr)

Abstract. A fine-scale source apportionment of PM$_{10}$ was conducted in three different urban sites (background, hypercenter, and peri-urban) within 15 km of the city in Grenoble, France using Positive Matrix Factorization (PMF 5.0) on measured chemical species from collected filters (24 h) from February 2017 to March 2018. To improve the PMF solution, several new organic tracers (3-MBTCA, pinic acid, phthalic acid, MSA, and cellulose) were additionally used in order to identify sources that are commonly unresolved by classic PMF methodologies. An 11-factor solution was obtained in all sites, including commonly identified sources from primary traffic (13 %), nitrate-rich (17 %), sulfate-rich (17 %), industrial (1 %), biomass burning (22 %), aged sea salt (4 %), sea/road salt (3 %), and mineral dust (7 %), and the newly found sources from primary biogenic (4 %), secondary biogenic oxidation (10 %), and MSA-rich (3 %). Generally, the chemical species exhibiting similar temporal trends and strong correlations showed uniformly distributed emission sources in the Grenoble basin. The improved PMF model was able to obtain and differentiate chemical profiles of specific sources even at high proximity of receptor locations, confirming its applicability in a fine-scale resolution. In order to test the similarities between the PMF-resolved sources, the Pearson distance and standardized identity distance (PD-SID) of the factors in each site were compared. The PD-SID metric determined whether a given source is homogeneous (i.e., with similar chemical profiles) or heterogeneous over the three sites, thereby allowing better discrimination of localized characteristics of specific sources. Overall, the addition of the new tracers allowed the identification of substantial sources (especially in the SOA fraction) that would not have been identified or possibly mixed with other factors, resulting in an enhanced resolution and sound source profile of urban air quality at a city scale.

1 Introduction

Atmospheric aerosols, or particulate matter (PM), are complex mixtures of particles from direct and indirect emissions (e.g., gas-to-particle conversion processes) that are from natural and anthropogenic sources in the atmosphere (Wilson and Spengler, 1996). The growing interest in ambient aerosol studies is driven by their impacts on health, air quality, and global climate (Colette et al., 2008; Horne and Dabdub, 2017; McNeill, 2017; Shiraiwa et al., 2017). Numerous epidemiological studies have established consistent associations between PM and various health diseases, espe-

cially cardiorespiratory illnesses (Brunekreef, 2005; Franchini and Mannucci, 2009; Langrish et al., 2012; Ostro et al., 2011; Willers et al., 2013). Once inhaled, PM notably has the capacity to generate reactive oxygen species (ROS), which leads to pro-inflammatory responses that can ultimately result in apoptosis (Ayres et al., 2008; Jin et al., 2018; Nel, 2005; Piao et al., 2018; Yang et al., 2018). Investigating the PM oxidative potential (OP) in light of its major emission sources in various urban environments can then provide valuable information to instigate air pollution abatement policies limiting health outcomes. However, spatially resolved PM source apportionment at a city scale remains a challenging task (Dai et al., 2020a, b; Pandolfi et al., 2020).

Receptor models demonstrated their ability to extract information by variable reduction techniques, especially in large datasets, in different branches of scientific research. In particular, the Positive Matrix Factorization (PMF) model is widely used in many studies to determine the contribution of emission sources in PM, based on the characterization of chemical tracers in a series of PM samples (Belis et al., 2014, 2020; Hopke, 2016; Pindado and Perez, 2011; Saeaw and Thepanondh, 2015; Weber et al., 2019). The option of refining source profiles by adding constraints have further improved the accuracy of identifying sources (Charron et al., 2019; Marmur et al., 2007; Weber et al., 2019; Zhu et al., 2018), especially when specific chemical species and unique tracers are included (Bullock et al., 2008; Wang et al., 2017b; Yan et al., 2017; Zhang et al., 2010). In fact, the PMF model has shown good strengths in both rural and urban environments (Pindado and Perez, 2011; Schauer and Cass, 2000); however, there are limited studies in cities at a fine-scale resolution that allows the assessment of local variabilities in a metropolitan area.

The city of Grenoble (France), with a complex topography and marked seasonal cycles of particulate pollution, offers interesting opportunities to explore the capability of PMF to resolve both the small spatial and large temporal scales of variabilities of the contribution of PM sources with the possibility of using additional tracers. Specific meteorological conditions, topography, and local sources impact the local PM chemistry in the atmosphere thereby requiring additional sources to properly scrutinize these local variations in urban environments. Further, previous works were already conducted in the area using extended PMF (Srivastava et al., 2018b; Weber et al., 2019), providing useful benchmark indicators.

The application of PMF requires to accurately consider a wide range of chemical components in PM, particularly for its organic fraction (Seinfeld and Pankow, 2003), consisting of complex mixtures especially in urban environments (Schauer and Cass, 2000; Zheng et al., 2004). In fact, around 80 % of organic matter (OM) generally remains unidentified at the molecular level (Chevrier, 2016; Golly et al., 2019) resulting in misclassification or several unapportioned sources of PM$_{10}$. Additionally, the difference in formation pathways of PM components may limit the identification of sources of PM, especially the secondary organic carbon (SOC) fraction, without the use of relevant organic tracers (Srivastava et al., 2018b; Wang et al., 2017b). Different organic tracers have already been integrated in previous PMF studies, allowing resolution of specific sources of organic aerosols that cannot be easily identified, such as primary biogenic aerosols and products of secondary processes in the atmosphere (Waked et al., 2014; Belis et al., 2019; Golly et al., 2019; Hu et al., 2010; Weber et al., 2019).

In particular, Srivastava et al. (2018b) were able to differentiate between different types of primary and secondary organic fractions at a Grenoble urban background site, after analysing about 150 organic markers (and selecting 25 of them for the final PMF run). Such studies are highly labour-intensive and often require the use of costly analytical devices and methods, whereas some of the missing key molecular markers might still be obtained using simpler and/or more targeted techniques. Moreover, the usefulness of these organic tracers in PMF analysis requires extensive methodological exploration, in terms of their applicability as source tracers considering the much lower variability of their concentrations compared to other traditional tracers.

In this paper, we present results of a study conducted over 1 year at three sites within 15 km of each other in the Grenoble metropolitan area within the framework of the Mobil'Air project (available in https://mobilair.univ-grenoble-alpes.fr/, last access: 2 November 2020). The sources of PM$_{10}$ were apportioned considering major chemical components contributing to the PM mass, including organic and elemental carbon, ions, a condensed set of commonly used organic markers (anhydride monosaccharides, polyols, MSA), and metals. Additional fit-for-purpose tracers, including free cellulose and several organic acids, were also added in the PMF input datasets to tackle specific sources that are difficult to discriminate using a traditional PMF dataset only. Results obtained from this improved PMF analysis were then used to investigate the spatial and seasonal variabilities in the source contributions for different urban typologies inside a metropolitan area. The overall outputs of this study could be of interest to policy makers in providing vital information for designing effective particulate matter control strategies including the setup of low emission zones and an opportunity to acquire more knowledge about the associations of these emissions with other emerging health-based metrics (e.g., OP of PM) at a city scale as presented in the companion paper (Borlaza et al., 2021).

2   Methodology

2.1   PM$_{10}$ sample collection

The metropolitan area of Grenoble, regarded as the capital of the French Alps, has a population of about 440 000 inhabi-
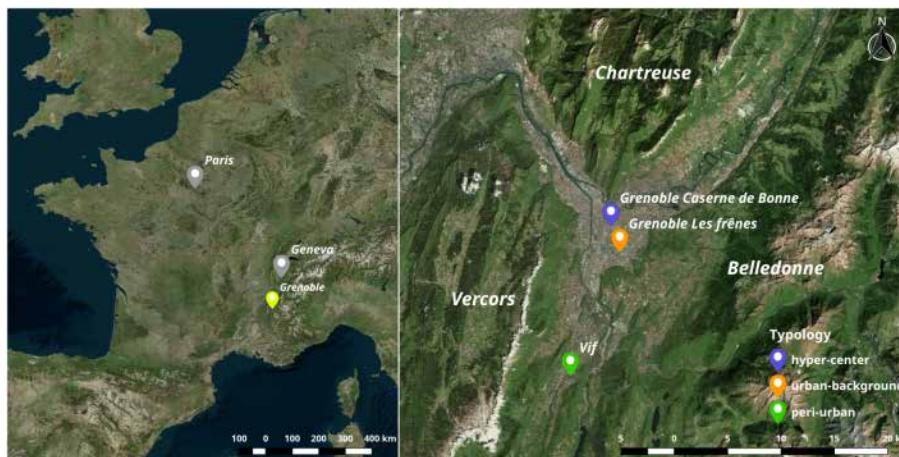
Figure 1. Grenoble, the city where the sampling was made, placed on a European map (left), and PM monitoring sites (right): Les Frênes or LF (background), Caserne de Bonne or CB (hyper-center), and Vif (peri-urban). Image credit: Bing™Aerial. © Microsoft.

tants. The city itself presents a low altitude range (between 204 and 600 m a.s.l.) but is located in an alpine environment (Fig. 1), surrounded by several mountain ranges, including Chartreuse (north), Vercors (south and west), and Belledonne (east). These mountains restrict the movement of air heavily affecting the local meteorology and favouring the development of atmospheric temperature inversions with entrapment of pollutants in the valley, particularly in the winter (Bessagnet et al., 2020). The topography within the Grenoble basin and seasonality of particulate air pollution in the city makes it an ideal location to explore both the small- and large-scale variabilities of PM sources During this study, a PM$_{10}$ sampling campaign was conducted in the Grenoble area at three sites selected to represent various urban typologies, including Les Frênes (LF, urban background site, 214 m a.s.l.), Caserne de Bonne (CB, urban hyper-center, 212 m a.s.l.), and Vif (peri-urban area, 310 m a.s.l.). These sites are all within a 15 km range from the city center. LF is a long-standing reference urban background site for the regional air quality monitoring network (Atmo Auvergne Rhône-Alpes), nearby a park at the outer fringe of the city. Vif is a peri-urban site, with suburban housings close to rural areas. However, this site could potentially receive industrial emissions from a nearby chemical industrial area (< 6 km) in the air flux within this north–south valley. Substantial influence of biogenic emissions could also be expected as this site is in between the foot of Vercors and Belledone national parks. Lastly, while in a pedestrian area, the site of CB is in the hyper-center of Grenoble and exposed to traffic emissions from the nearby boulevards.

The daily (24 h) PM$_{10}$ sampling collection was conducted from 28 February 2017 to 10 March 2018 (starting at 00:00 LT) with an average 3 d sampling interval. A total of 125, 127 and 127 samples were collected during this year-long campaign at LF, CB, and Vif, respectively.

The PM$_{10}$ collection was performed using high-volume samplers (Digitel DA80, 30 m^3 h^{-1}) onto 150 mm-diameter pure quartz fibre filters (Tissu-quartz PALL QAT-UP 2500 diameter 150 mm). All filter-handling procedures of filters were strictly under quality control assurance procedures to avoid any possible contamination. In particular, filters were preheated at 500 °C for 12 h before use to avoid organic contamination. At least 20 field blank filters were collected at each site to determine detection limits (DL) and to check for the absence of contamination during sample transport, setup, and recovery. After particle collection, filter samples were wrapped in aluminium foil, sealed in zipper plastic bags, and stored at < 4 °C until further chemical analysis. Complementary measurements at the sampling sites notably included the total PM$_{10}$ mass concentration measured using tapered element oscillating microbalances equipped with filter dynamics measurement systems (TEOM-FDMS) (Grover, 2005).

2.2 Classical set of chemical analyses

Sampled filters were subjected to various chemical analyses for the quantification of the major chemical constituents and specific chemical tracers of sources needed for PMF studies.

The carbonaceous fractions (organic carbon (OC) and elemental carbon (EC)) were analysed with a Sunset Lab analyser (Aymoz et al., 2007; Birch and Cary, 1996) using the EUSAAR2 thermo-optical protocol (Cavalli et al., 2010). Total organic matter (OM) in daily ambient aerosols were estimated by multiplying the OC mass by a fixed conversion factor of 1.8 based on findings obtained from previous studies (Favez et al., 2010; Putaud et al., 2010).

A solid/liquid extraction was performed on 11.34 cm^2 punches soaked in a 10 mL of ultra-pure water under vortex agitation for 20 min. The extract was then filtered with a 0.25 µm porosity Acrodisc (Milipore Millex-EIMF) filter. The major ionic components were measured by ion chro-

matography (IC) following a standard protocol described in Jaffrezo et al. (1998) and Waked et al. (2014), using an ICS3000 dual-channel chromatograph (Thermo-Fisher) with AS11HC column for the anions and CS12 for the cations. This technique allowed the quantification of sodium (Na$^+$), ammonium (NH$_4^+$), potassium (K$^+$), magnesium (Mg^{2+}), calcium (Ca^{2+}), chloride (Cl$^-$), nitrate (NO$_3^-$), sulfate (SO$_4^{2-}$), and methane sulfonic acid (MSA).

Furthermore, anhydro-sugars and saccharides were analysed by high-performance liquid chromatography with pulsed amperometric detection (HPLC-PAD), using a Thermo-Fisher ICS 5000$^+$ HPLC equipped with 4 mm diameter Metrosep Carb 2 × 150 mm column and 50 mm precolumn in isocratic mode with 15 % of an eluent of sodium hydroxide (200 mM) and sodium acetate (4 mM) and 85 % water, at 1 mL min^{-1}. This method notably allowed the quantification of anhydrous saccharides (levoglucosan and mannosan), polyols (arabitol and mannitol), and glucose as tracers of biomass burning and primary biogenic aerosols (Samaké et al., 2019b; Waked et al., 2014).

Finally, major and trace elements were analysed after mineralization of a 38 mm diameter punch of each filter, using 5 mL of HNO$_3$ (70 %) and 1.25 mL of H$_2$O$_2$ during 30 min at 180 °C in a microwave oven (microwave MARS 6, CEM). The analysis of 18 elements (Al, As, Ba, Cd, Cr, Cu, Fe, Mn, Mo, Ni, Pb, Rb, Sb, Se, Sn, Ti, V, and Zn) was performed on this extract using inductively coupled plasma mass spectroscopy (ICP-MS) (ELAN 6100 DRC II PerkinElmer or NEXION PerkinElmer) in a way similar to that described by (Alleman et al., 2010).

The procedures for filter sampling and chemical analyses have been performed following the recommendations of related EN standards (i.e., EN 12341, EN 14902, EN 16909, EN 16913) (Favez et al., 2021). Moreover, quality control of the chemical speciation analyses includes chemical mass closure as presented in Sect. S2. It should also be noted that our group successfully participates in regular inter-laboratory comparison exercises for OC and EC within ACTRIS and in EMEP (European Monitoring and Evaluation Programme) for ions analysis.

2.3 Additional set of analyses of organic tracers

2.3.1 Organic acids

The analysis of a large array of organic acids (including pinic and phthalic acids, and 3-MBTCA) was conducted using the same water extracts as for IC and HPLC-PAD analyses. In brief, this was performed by HPLC-MS (GP40 Dionex with a LCQ-FLEET Thermos-Fisher ion trap), with negative mode electrospray ionization. The separation column is a Synergi 4 μm Fusion – RP 80A (250 × 3 mm ID, 4 μm particle size, from Phenomenex). An elution gradient was optimized for the separation of the compounds, with a binary solvent gradient consisting of 0.1 % formic acid in acetoni-

trile (solvent A) and 0.1 % aqueous formic acid (solvent B) in various proportions during the 40 min analytical run. Column temperature was maintained to 30 °C. Eluent flow rate was 0.5 mL min^{-1}, and injection volume was 250 μL. Calibrations were performed for each analytical batch with solutions of authentic standards. All standards and samples were spiked with internal standards (phthalic-3,4,5,6-d^4 acid and succinic-2,2,3,3-d^4 acid). The calculation of the final atmospheric concentrations was corrected with the concentrations of internal standards and of the procedural blanks, taking also into account the extraction efficiency varying between 76 % and 116 % (depending on the acid).

2.3.2 Cellulose

The concentration of cellulose within PM$_{10}$ samples was quantified based on a protocol improving the procedure proposed by Kunit and Puxbaum (1996). Cellulose was extracted from the filter in an aqueous solution, which was then processed in several solutions of enzymes in order to breakdown the cellulose into glucose units. Resulting glucose concentration was quantified using an HPLC-PAD technique. To do so, a 21 mm diameter punch was first extracted for 40 min using an ultrasound bath in 3 mL of an aqueous solution with thymol buffer (pH 4.8). Then two enzymes solutions (cellulase (Sigma Aldrich, C2730) with 20 μL of an aqueous solution at 70 units g^{-1}) and glucosidase (Sigma Aldrich, 49291), with 60 μL of an aqueous solution at 5 units g^{-1}) are added into the solution. The solution was then incubated at 50 °C for 24 h for the hydrolysis to occur. The hydrolysis is stopped by placing the solution in an oven at 100 °C for 45 min. The solution was then centrifuged (7000 rpm) for 15 min, and carefully extracted out using a syringe before being analysed with an HPLC-PAD instrument. The procedural blanks are greatly improved when the enzymes stock solutions are filtered to lower their glucose content. This is performed with a series of cleaning steps ($n = 10$) by tangential ultrafiltration in a Vivaspin 15R tube at 7000 rpm in Milli-Q water.

The HPLC-PAD (Dionex DX500) is equipped with a Metrohm column (250 mm long, 4 mm diameter), with an isocratic run of 40 min with the eluents A (50 %, 18 mM NaOH), B (25 %, 100 mM NaOH + 150 mM NaAc), and C (25 %, 220 mM NaOH). Column temperature is maintained at 30 °C. Eluent flow rate is 1 mL min^{-1}, and injection volume is 250 μL. Each analytical batch also includes standard glucose solutions as well as standard cellulose solutions (using 20 μm beads, Sigma Aldrich, S3504) that have been processed like the real samples in order to determine the specific efficiency of the cellulose-to-glucose enzymatic conversion for each batch. The final calculation of the atmospheric concentration of the free cellulose takes this conversion efficiency into account. It varied according to the batch, generally ranging from 65 % to 80 %. The calculation of the cellulose concentration also takes into account the initial concentrations of atmospheric glucose of each sample, determined

in parallel with the HPLC-PAD analysis of sugars and polyols as described above. Finally, field and procedural blanks are also taken into account.

2.4 Source apportionment

2.4.1 PMF input dataset

Source apportionment of PM$_{10}$ was conducted using the United States Environmental Protection Agency (US-EPA) software PMF 5.0 (Norris et al., 2014), aiming at the identification and quantification of the major sources of PM$_{10}$ for the three urban sites in the Grenoble basin. Briefly, PMF is based on the factor analysis technique (Paatero and Tapper, 1994) applying a weighted least-squares fit algorithm allowing the resolution of Eq. (S1) (in the Supplement). In our study, 35 chemical species were used as input variables, namely OC*, EC, ions (Na$^+$, K$^+$, NH$_4^+$, Mg^{2+}, Ca^{2+}, NO$_3^-$, SO$_4^{2-}$ and Cl$^-$), trace metals (Al, As, Cd, Cr, Cu, Fe, Mn, Mo, Ni, Pb, Rb, Sb, Se, Sn, Ti, V and Zn) and organic tracers (MSA, levoglucosan, mannosan, polyols (sum of arabitol and mannitol), pinic acid, 3-MBTCA, phthalic acid, and cellulose), as summarized in Table S1 in the Supplement. We assumed that arabitol and mannitol originated from the same source, and hence combined them into one component labelled as "polyols" (Samaké et al., 2019a). In order to avoid double counting of carbon mass, OC* was calculated as the difference between total OC and the quantity of C atoms contained in the different organic markers included in the PMF input data matrix (as detailed in Eq. S2). The uncertainties of the input variables were calculated using Eq. (S3) (Gianini et al., 2012). Finally, the species displaying a signal-to-noise ratio (S/N) lower than 0.2 were discarded and those with S/N between 0.2 and 2 were classified as "weak" variables (and then down-weighted applying 3-fold uncertainties).

2.4.2 Set of constraints

Since mixing issues between factors are inherent to PMF (i.e., collinearity due to meteorological conditions) and to possible rotational ambiguity in the solution, we applied a set of constraints to the selected best base case solutions thanks to the ME-2 solver (Paatero, 1999). The constraints used were similar to that of Weber et al. (2019), who applied a minimum set of constraints to a large series of data sets within the SOURCE program. We also added specific constraints for the traffic factor, derived from a previous study in Grenoble dedicated to traffic emissions (Charron et al., 2019), as summarized in Table 1. These constraints were applied similarly to the data sets from the three sites. This allows the orientation of the PMF solution towards more stable and environmentally realistic profiles.

2.4.3 Criteria for a valid solution

Solutions with a total number of factors between 7 and 12 were tested for the determination of the base cases. During factor selection, the Q/Q_{exp} ratio (< 1.5), the geochemical interpretation of the factors, the weighted residual distribution, and the total reconstructed mass were evaluated. Finally, the optimal solutions obtained for each urban site was subjected to error estimation to ensure stability and accuracy of the solutions, using displacement (DISP) and bootstrapping (BS) methods. The DISP analysis evaluates that no swapping had occurred in any of the factors. Solutions with > 80 out of 100 BS mapped factors were considered appropriate solutions. The final retained optimal solutions after the application of constraints fulfilled the recommendations of the European guide on air pollution source apportionment with receptor models (Belis et al., 2014). The sensitivity of the solutions to the applied constraints was also carefully evaluated by comparison between the base and constrained cases. More information about the source apportionment methodology is provided in the SI.

2.4.4 Similarity assessment

A test of similarity between source profiles, based on their specific chemical relative mass composition at each site, was performed by comparing the Pearson distance (PD) and standardized identity distance (SID). This allows the evaluation of the variability of the solutions across these different urban environments. The PD and SID were calculated using Eq. (S4) (Belis et al., 2015).

The PD metric represents the sensitivity of a chemical profile based on the differences in the major mass fractions of PM, whereas the SID represents the sensitivity to all components (hence taking into account trace species). Homogenous profiles that are stable over different site types are expected to have PD < 0.4 and SID < 1.0 (Pernigotti and Belis, 2018). Conversely, factors outside of this range are considered to have heterogeneous profiles.

2.4.5 Estimation of the contribution uncertainties

The BS profiles uncertainties for the obtained solutions are presented in Sect. S3, in the form of mean±std of the 100 BS for all sites. As PMF5.0 does not directly output this to the user, we provided an estimate of the contribution uncertainties based on the method presented in Weber et al. (2019). During the BS estimation, both the **G** and **F** matrices are available; however, only the **F** matrix is given back to the user (the **G** matrix being used internally to map the different profiles). Hence, the daily contributions of each of the species are estimated using

$$\mathbf{X}_{BSi} = \mathbf{G}_{ref} \times \mathbf{F}_{BSi}, \tag{1}$$

where $\mathbf{F}_{BSi}$ is the profile of the bootstrap i, and $\mathbf{X}_{BSi}$ is the time series of each species according the reference contribu-

Table 1. Summary of the applied chemical constraints on source-specific tracers in the PMF factor profiles.

Factor profile	Element	Type	Value
Biomass burning	Levoglucosan	Pull up maximally	(% dQ 0.50)
Biomass burning	Mannosan	Pull up maximally	(% dQ 0.50)
Primary biogenic	Levoglucosan	Set to zero	0
Primary biogenic	Mannosan	Set to zero	0
Primary biogenic	Polyols	Pull up maximally	(% dQ 0.50)
Primary biogenic	EC	Pull down maximally	(% dQ 0.50)
MSA-rich	MSA	Pull up maximally	(% dQ 0.50)
MSA-rich	Levoglucosan	Set to zero	0
MSA-rich	Mannosan	Set to zero	0
MSA-rich	Polyols	Pull down maximally	(% dQ 0.50)
MSA-rich	EC	Pull down maximally	(% dQ 0.50)
Nitrate-rich	Levoglucosan	Set to zero	0
Nitrate-rich	Mannosan	Set to zero	0
Mineral dust	Ti	Pull up maximally	(% dQ 0.50)
Primary traffic	Levoglucosan	Set to 0	0
Primary traffic	Mannosan	Set to 0	0
Primary traffic*	Cu	Pull up maximally	(% dQ 0.50)
Primary traffic*	Fe	Pull up maximally	(% dQ 0.50)
Primary traffic*	Sn	Pull up maximally	(% dQ 0.50)
Primary traffic*	Ca^{2+}	Pull down maximally	(% dQ 0.50)
Primary traffic	Cu/Fe	Set to value	0.046 (% dQ 0.50)
Primary traffic	Cu/Sn	Set to value	5.6 (% dQ 0.50)
Primary traffic	Cu/Sb	Set to value	12.6 (% dQ 0.50)
Primary traffic	Cu/Mn	Set to value	5.7 (% dQ 0.50)
Primary traffic	OC*/EC	Set to value	0.44 (% dQ 0.50)

* Only applied in the Vif (peri-urban) site.

tion G_{ref} and the bootstrap run F_{BSi}. Similarly, the DISP contribution uncertainties are given by the reference contribution G multiplied by the lower and upper limits of the DISP result for each species.

3 Results and discussion

3.1 General evolution of concentrations of PM$_{10}$ and chemical species

The daily PM$_{10}$ mass concentrations at the three measurement sites, determined with the TEOM-FDMS for the dates of filter sampling, ranged from 3 to 61 µg m^{-3} with an overall average of 14 ± 9 µg m^{-3} during the sampling period. Average PM$_{10}$ levels were the highest at the urban hypercenter site (CB) (16 ± 10 µg m^{-3}), followed by the urban background site (LF) (14 ± 8 µg m^{-3}), and the peri-urban site (Vif) (13 ± 9 µg m^{-3}). Annual averages of PM$_{10}$ mass concentrations and chemical compositions at all sites and at individual urban sites are shown in Table S2. The sites in this study showed minimal exceedances of the current PM$_{10}$ European limit value of 40 µg m^{-3} (3.7 %, 1.6 %, and 1.6 % of measurement days at the LF, CB, and Vif sites, respectively). Most of these exceedances occurred during the winter season

indicating the necessity to additionally implement season-specific regulations for PM$_{10}$ emission reductions. Organic matter (OM) was the largest contributor in PM$_{10}$ and accounted for 54 %, 51 %, and 56 % of mass concentration on an annual basis in LF, CB, and Vif, respectively. This was followed by contributions from the major inorganic species (NH$_4^+$, NO$_3^-$, and SO$_4^{2-}$), suggesting strong influence from secondary inorganic aerosol (SIA) that are generally associated with long-range transport of pollutants or the occurrence of a small-scale thermal inversion within the Grenoble basin. An extensive description of the PM$_{10}$ chemistry in the Grenoble basin has already been presented in Srivastava et al. (2018b) for the years 2013–2014 at the LF site. Our results showed notable similarities for most chemical species for the year 2017–2018, especially in terms of seasonal variations and respective contribution of chemical species to PM$_{10}$ mass concentrations. Therefore, we will only describe these aspects briefly in this paper.

First, the time series analysis of PM$_{10}$ and its chemical composition in the Grenoble basin during the sampling period showed mild to strong seasonal trends. Part of it can be attributed to the atmospheric dynamics in the area given its alpine environment resulting in atmospheric temperature inversions that are especially common in winter. In the absence of strong winds during the winter season (especially during

anti-cyclonic periods), higher concentrations of air pollutants could be expected. Indeed, PM$_{10}$ concentrations were higher during the colder months (October to April) with an average of $17 \pm 10\,\mu\text{g}\,\text{m}^{-3}$ and lower during the warmer months (May to September) with an average of $10 \pm 4\,\mu\text{g}\,\text{m}^{-3}$.

We observed a strong seasonality for some chemical species with higher concentrations during the colder months including OC*, EC, K$^+$, NO$_3^-$, NH$_4^+$, levoglucosan, mannosan, and phthalic acid. These species are commonly associated with primary emissions during the process of biomass burning (OC, EC, K$^+$, levoglucosan, mannosan) and secondary atmospheric processing (NO$_3^-$, NH$_4^+$, phthalic acid). Alternatively, specific species with higher concentrations during warmer months include MSA, polyols, 3-MBTCA, and pinic acid. These species are known to be products of a wide range of photochemical reactions in the atmosphere partly formed by OH-initiated oxidation (Atkinson and Arey, 1998; Szmigielski et al., 2007) and can be explained by enhanced photochemical production due to an increase in temperature-dependent hydroxyl radical (OH) concentration. A summary of temporal evolutions of the concentration for some species including SO$_4^{2-}$, Cu, cellulose, polyols, 3-MBTCA, pinic acid, and phthalic acid is shown in Fig. 2.

Second, the Pearson correlation coefficients of the temporal evolution of each species across sites is presented in Fig. 3. Similarity of temporal trends and strong correlations of PM$_{10}$ components between our three sites indicates the influence of large-scale transport processes or possible uniform distribution of some emission sources in the Grenoble area. Further, the accumulation and removal processes of the PM may be driven by similar season-specific environmental conditions at a local scale. A strong correlation was observed in OC*, EC, ions, polyols, levoglucosan, mannosan, 3-MBTCA, phthalic acid, and pinic acid between sites suggesting similar origins and atmospheric processes affecting the concentrations of these species. The three sites seem to be equally impacted by long-range transport since concentration of SO$_4^{2-}$ appears almost identical. We also clearly see relatively similar temporal trends for the organic acids (MSA, pinic, and 3-MBTCA). Notably, we also observed an important episode in phthalic acid in late February 2018 affecting all the three sites. An extensive discussion on the formation processes of anthropogenic SOA in high-concentration events was already provided in Srivastava et al. (2018b). However, this new observation brings in the hypothesis that these processes may take place specifically due to heterogeneous chemistry when associated with fog episodes, as can be observed by local web cams over the city (discussed in answers to reviewers). Conversely, cellulose and most metal species showed weak to mild correlations between sites, possibly indicating that the sources of these species are highly localized, with a potential impact that is variable at a city scale. Particularly, cellulose presents similar order of magnitude at the three sites but presents higher concentration at CB,

Table 2. Summary of PMF-resolved sources and their specific tracers.

Identified factors	Specific tracers
Biomass burning	Levoglucosan, mannosan, K$^+$, Rb, Cl$^-$
Primary traffic	EC, Ca^{2+}, Cu, Fe, Sb, Sn
Nitrate-rich	NO$_3^-$, NH$_4^+$
Sulfate-rich	SO$_4^{2-}$, NH$_4^+$, Se
Mineral dust	Ca^{2+*}, Al, Ti, V
Sea/road salt	Na$^+$, Cl$^-$
Aged sea salt	Na$^+$, Mg^{2+}
Industrial	As, Cd, Cr, Mn, Mo, Ni, Pb, Zn
Primary biogenic	Polyols, cellulose
MSA-rich	MSA
Secondary biogenic oxidation	3-MBTCA, pinic acid

* Vif site did not have high loadings of Ca^{2+} species in this factor.

especially during winter. A few metals only showed strong correlations between LF and CB but not with Vif, such as Al, Cu, Fe, Rb, and Sb, which are tracers of road transport activity or biomass burning emissions. Specifically, Cu concentrations are similar at the three sites during summer but present significantly lower concentration in Vif compared to the two urban sites of CB and LF during winter.

3.2 PM$_{10}$ source apportionment

In the following sections, a description of the best PMF solution obtained after application of constraints is provided for each of the three sites, together with a discussion about the factors that are associated with the added organic tracers (MSA, polyols, cellulose, pinic and 3-MBTCA acids). The presentation of error estimations, chemical profiles, and temporal evolutions of the PMF-resolved sources, and the discussion about the more classical factors can be found in Sect. S3.

3.2.1 General description of the solutions

The PMF model was applied independently on the data set of each three sites, using 35 chemical atmospheric compounds in each site. The constrained solutions for each site consist of 11 factors, including common factors such as primary traffic, biomass burning, nitrate-rich, sulfate-rich, aged sea salt, sea/road salt, and mineral dust. Also, with the use of biogenic tracer species, we identified a primary biogenic factor and a MSA-rich factor. These factors are similarly determined in Weber et al. (2019) for each of 15 sites in France. We also determined a metal-rich factor, identified as an industrial factor, accounting for a very small part of the PM$_{10}$ mass. Finally, using new organic proxies (pinic and 3-MBTCA acids), we identified a secondary biogenic oxidation factor that is rarely described in other PMF studies. Table 2 shows a synthesis of the tracers used to identify these 11 PMF-resolved factors that are found at each of the three sites.
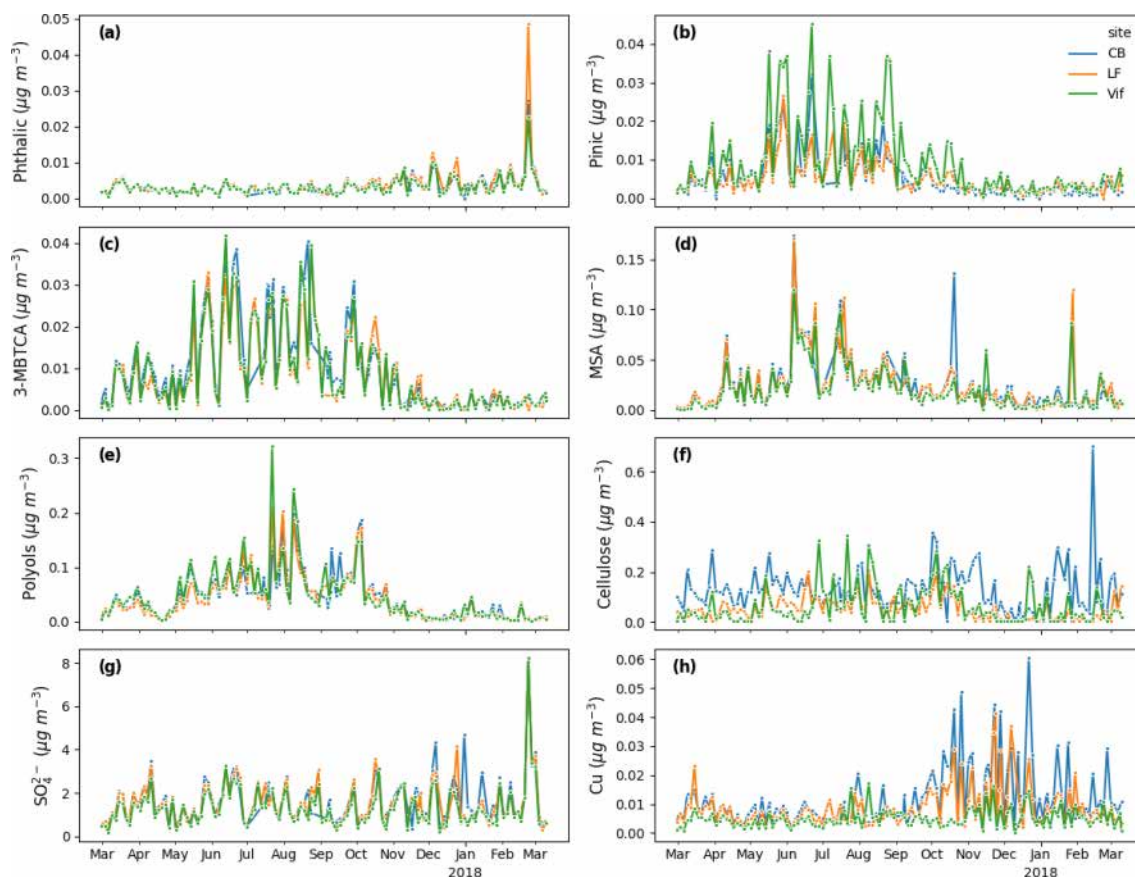
Figure 2. Temporal evolutions of **(a)** phthalic acid, **(b)** pinic acid, **(c)** 3-MBTCA, **(d)** MSA, **(e)** polyols (arabitol + mannitol), **(f)** cellulose, **(g)** SO$_4^{2-}$ and **(h)** Cu in the three urban sites in the Grenoble basin (LF in orange, CB in blue, and Vif in green).
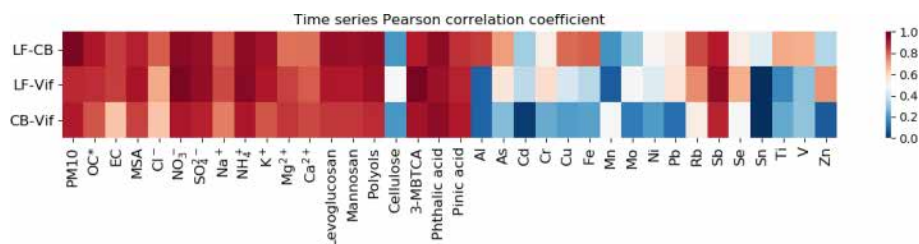

Figure 3. Concentration time series Pearson correlation coefficient of PM$_{10}$ and its chemical composition between LF and CB (LF-CB), LF and Vif (LF-Vif), and CB and Vif (CB-Vif).

Other solutions with fewer or greater number of factors were also investigated but these solutions were less defined, and factor merging was often observed. The reconstructed PM$_{10}$ contributions from all sources with measured PM$_{10}$ concentration showed very good mass closure in all sites (LF: $r = 0.99$, $n = 125$, $p < 0.05$; CB: $r = 0.99$, $n = 126$, $p < 0.05$; and Vif: $r = 0.99$, $n = 126$, $p < 0.05$) indicating very good model results.

This result is in line with a previous study in the city of Grenoble (Srivastava et al., 2018b) but with slight improvements in the PM$_{10}$ mass closure (from $r = 0.93$ to $r = 0.99$).

A complete comparison of the PMF-resolved sources between the two studies is presented and discussed in Sect. S4. The two sets of results are in good agreement, despite the samples being collected 4 years apart. There were several identified sources that are similar in both studies such as biomass burning, primary traffic, mineral dust, aged sea salt, sulfate- and nitrate-rich (identified collectively as secondary inorganics in Srivastava et al., 2018b), and primary biogenic (identified as fungal spores and plant debris in Srivastava et al., 2018b). Additionally, due to a number of differences in the input variables used, there are some sources that are

completely unique to each study. In particular, the sources that we have uniquely identified are industrial, sea/road salt, MSA-rich, and secondary biogenic oxidation sources. Conversely, Srivastava et al. (2018b) have uniquely identified two SOA sources: biogenic SOA and anthropogenic SOA. It can be argued that the secondary biogenic oxidation source (11 %) in our study and the biogenic SOA (12 %) in Srivastava et al. (2018b) are in some way similar, although different tracers were used to identify them. Particularly, Srivastava et al. (2018b) identified the biogenic SOA source with high contributions from α-methylglyceric acid (α-MGA and 2-methylerythritol (2-MT) that are isoprene oxidation products and hydroxyglutaric acid (3-HGA), an oxidation product from α-pinene. On the other hand, our study identified the secondary biogenic oxidation source with high contributions from 3-MBTCA and pinic acid (essentially from α-pinene oxidation). While not uniquely identified in our study, the contributions of phthalic acid in several common anthropogenic-derived sources (sulfate- and nitrate-rich) can also mark the potential contributions from anthropogenic SOA sources. Finally, the considerable economic advantage in the specific organic tracers used in our study, in terms of the type of chemical analyses performed, could assist future studies utilizing organic species in PMF.

It is also important to note that, although still in the acceptable range, the sulfate-rich factor obtained in our PMF results yielded the most BS unmapped factors amongst the PMF-resolved factors (up to 25 % for the CB site). This may be the sign of possible mixing of different processes/sources in this factor.

3.2.2   PM$_{10}$ contribution

Biomass burning (17 %–26 %), sulfate-rich (16 %–18 %), and nitrate-rich (14 %–17 %) sources were the highest contributors to the total PM$_{10}$ mass on a yearly average in the Grenoble basin. Primary traffic (12 %–14 %) and secondary biogenic oxidation (8 %–11 %) sources also contributed a relevant amount. Figure 4 presents a comparison of the source contributions in each site based on mass concentration (in µg m^{-3}). These results are in line with recent studies leading to anthropogenic and SOA sources heavily influencing urban air pollution in western Europe (Daellenbach et al., 2019; Golly et al., 2019; Pandolfi et al., 2020; Srivastava et al., 2018b; Weber et al., 2019). The most notable difference across all sites is the sharp decrease in mineral dust in Vif compared to the other two urban sites, and this is discussed further in Sect. 3.4.1.

3.2.3   MSA-rich

This factor is identified with a high loading of MSA, a known product of oxidation of dimethylsulfide (DMS), commonly described as resulting from marine phytoplankton emissions (Chen et al., 2018; Li et al., 1993). Other chemical species

with significant concentrations in this factor include sulfate and ammonium. Although a very useful tracer of marine biogenic sources, MSA showed in our series only weak to mild correlations with ionic species from marine aerosols such as Na$^+$ (r: 0.2–0.3) and Mg^{2+} (r: 0.3–0.4). This suggests potential emissions originating from terrestrial biogenic sources instead, which has been similarly suggested before (Bozzetti et al., 2017; Golly et al., 2019), and/or from forest biota (Jardine et al., 2015; Miyazaki et al., 2012). On an annual scale, this factor accounted for 2 %–4 % of the total mass of PM$_{10}$ and shows a strong seasonality with highest contributions during summer, reaching up to 53 %, 57 %, 52 % of the total PM$_{10}$ mass on some specific days in LF, CB, and Vif, respectively. The similarity in the temporal distribution across sites, as shown in Fig. S3.8, especially the summer peaks, could be linked to the influence of long-range transport of pollutants in the MSA-rich factor.

3.2.4   Primary biogenic

The primary biogenic factor was identified with high loadings of both polyols and cellulose (see Fig. 5). Polyols (represented by the sum of arabitol and mannitol) are known as tracers of primary biological aerosols from fungal spores and microbes (Bauer et al., 2002; Igarashi et al., 2019). Polyols has been used in several studies as a tracer of biogenic sources, contributing in France within a range of 5 %–9 % of PM$_{10}$ on a yearly average (Samaké et al., 2019b; Srivastava et al., 2018b; Waked et al., 2014; Weber et al., 2019). Cellulose is a potential macro-tracer for plant debris from leaf litter and seed production (Kunit and Puxbaum, 1996; Puxbaum, 2003) that is very rarely used in source apportionment studies as of today. It can represent a large fraction of the PM mass in the coarse mode (Bozzetti et al., 2016), and it represents up to 6 % during the warm season in the Vif site.

A strong correlation was found in the temporal evolution of polyols across the three sites in our study indicative of large-scale impact of sources for these species (Samaké et al., 2019b). Conversely, cellulose concentrations present only weak correlations across the three sites, possibly indicating that the influence of the sources of this species might be more local. Although polyols and cellulose are both tracers of primary biogenic sources, only a rather mild correlation ($r = 0.5$) was found between these two tracers, with seasonality of their concentrations being slightly different (Fig. 2). It shows that the processes and the sources are probably distinct for the two sets of chemical species. However, the PMF is not able to separate them, and this factor includes most of the cellulose (58 %, 51 %, and 74 % in LF, CB, and Vif, respectively), and also most of the polyols (99 %, 90 %, and 83 % in LF, CB, and Vif, respectively). The remaining fraction of cellulose concentrations was included in the mineral dust factor in LF and CB, and in the primary traffic factor in Vif, suggesting the possibility of resuspension processes for this compound (see the SI for details). We can also note that
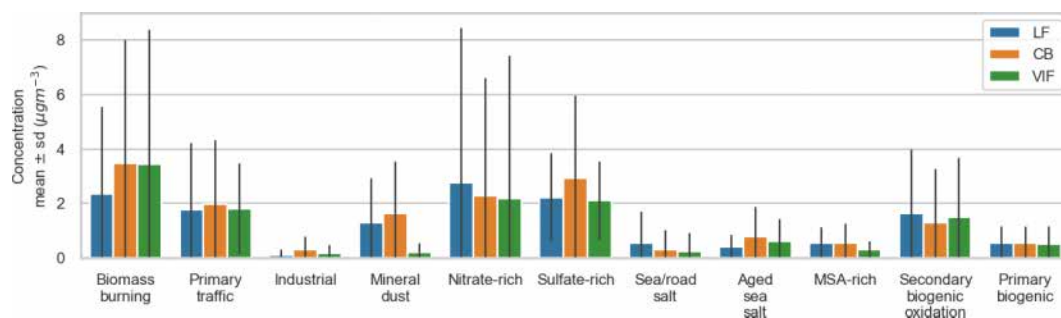
Figure 4. Factor contributions in µg m⁻³ for the three sites (LF: blue, CB: orange, Vif: green). Bar plots depict the mean annual value and the standard deviation of daily variations.

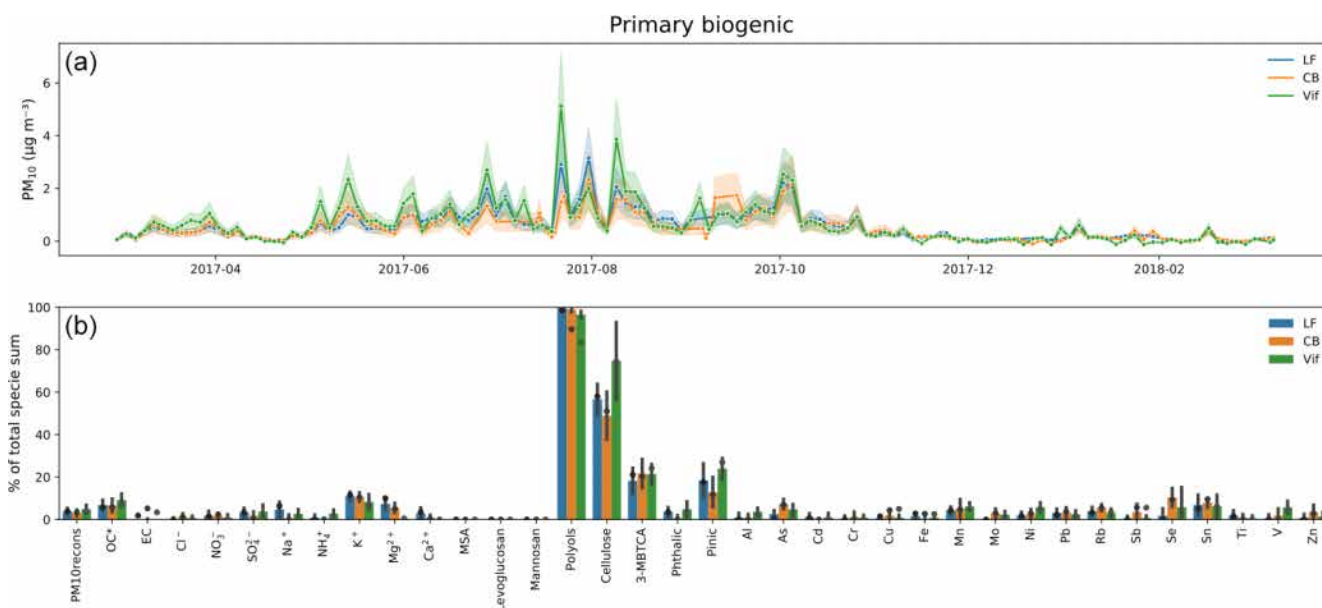**Figure 5.** Primary biogenic factor for the three urban sites. **(a)** Contribution to PM₁₀ given the mean and standard deviation of the 100 BS. **(b)** Percentage (%) of each species apportioned by this factor (dots refer to the constrained run, bar plots refer to the mean, and error bars refer to the standard deviation of the 100 BS).

the cellulose was not at all apportioned in the biomass burning factor, an indication that it may not be emitted by this source.

Despite their slightly different origins, the PMF analysis captures the combined contribution of polyols and cellulose to a factor that can be termed "primary biogenic sources". In this study, this factor accounted for 3 %–4 % of the total mass of PM₁₀ on an annual scale, and a strong seasonality was observed, with up to 18 % (in LF), 8 % (in CB), and 17 % (in Vif) of the total PM₁₀ mass on average in summer, with specific days reaching up to 60 % of PM₁₀ for example at the Vif site (see Fig. 5). These temporal variations are consistent with higher biological activity (increased production of fungal and fern spores and pollen grains) in this season due to increase in temperature and humidity (Graham et al., 2003; Verma et al., 2018). This may also be attributed to an increased plant metabolic activity (production of plant debris

from decomposition of leaves) and the proximity to forested and agricultural areas of the sampling sites (Gelencsér et al., 2007; Puxbaum, 2003). Finally, one can note that the chemical profiles also include some fractions of the tracers from secondary biogenic production (3-MBTCA and pinic acid), indicative of some degree of mixing between primary and secondary biogenics.

3.2.5 Secondary biogenic oxidation

The secondary biogenic oxidation factor was identified with high loadings of 3-MBTCA and pinic acids (see Fig. 6). Both tracers of this factor are known to be products of secondary oxidation processes of alpha-pinene from various biogenic origins. As suggested by the nearly identical mass fraction determined in Srivastava et al. (2018b) at the same site, this factor may also contain some PM resulting from the oxida-
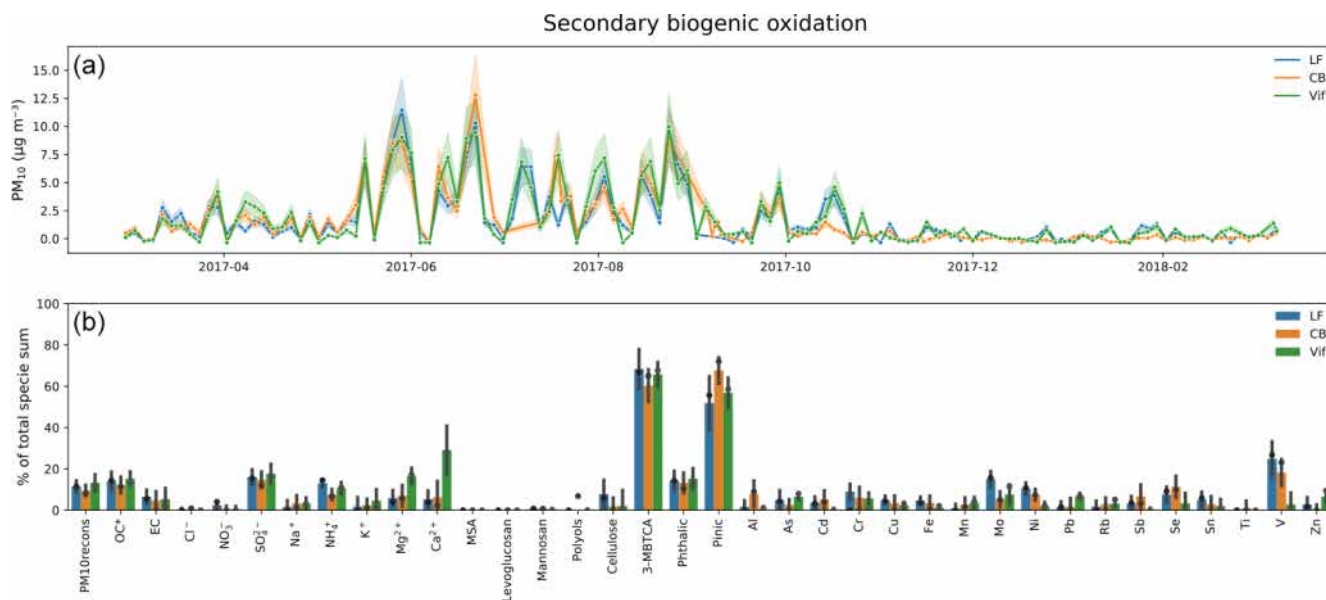
Figure 6. Secondary biogenic oxidation factor for the three urban sites. **(a)** Contribution to PM$_{10}$ given the mean and standard deviation of the 100 BS. **(b)** Percentage (%) of each species apportioned by this factor (dots refer to the constrained run, bar plots refer to the mean, and error bars refer to the standard deviation of the 100 BS).

tion of isoprene epoxydiols (IEPOX) (Surratt et al., 2010; Zhang et al., 2017) that may present a rather similar seasonality (Budisulistiorini et al., 2013, 2016), but this is still an open question.

The apportionment of such a factor is not commonly achieved in receptor modeling using offline tracers (van Drooge and Grimalt, 2015; Heo et al., 2013; Hu et al., 2010; Srivastava et al., 2018a). On an annual scale in our study, this factor accounted for 8 %–11 % of the total mass of PM$_{10}$, but can be as high as 58 % (11 µg m^{-3}) on specific days (see Fig. 6a). The strong correlation between 3-MBTCA and pinic acids suggests similarity of origin of the secondary biogenic oxidation factor in the Grenoble area, despite inter-site correlations for 3-MBTCA (older oxidation state of alpha-pinene, hence more homogeneous at the city scale) being larger than that for pinic acid (former oxidation product, less homogeneous). Although significant portions (56 %–72 %) of these species (3-MBTCA and pinic acids) are in this secondary biogenic oxidation factor, there are still relevant contributions in other factors, including primary biogenic, sulfate- and nitrate-rich, aged sea salt, and MSA-rich. Conversely, the presence of phthalic acid contribution in this factor (around 10 % of its concentration), which could be emitted directly from biomass burning or formed during secondary processing from anthropogenic emissions (Hyder et al., 2012; Kleindienst et al., 2007; Wang et al., 2017a; Yang et al., 2016), also suggests that this factor has anthropogenic influence. All of these indicate that the PMF process did not deliver a pure secondary biogenic oxidation factor, either due to data pro-

cessing limitation or because of real mixing of these sources in the PM.

3.3 Re-assignment of factors thanks to the new proxies

3.3.1 Importance of the new proxy for factor identification

With the use of these additional organic tracers, there are several added information drawn from the results of the PMF model. First, the notable contributions of phthalic acid in several sources could further confirm the mixing influence of anthropogenic processes in various sources of PM$_{10}$ such as sulfate- and nitrate-rich but also with secondary biogenic oxidation sources. Second, adding 3-MBTCA and pinic acids in the input variables allowed the identification of a significant secondary biogenic oxidation factor that is generally difficult to identify with PMF studies of offline samples. Comparisons already started with the factors obtained by AMS studies (Vlachou et al., 2018), but more work remains to be done in order to evaluate their proper correspondence.

3.3.2 Comparison with a "classic" PMF solution

In order to quantify the added value and the changes brought in by the additional tracers, a reference PMF using a chemical dataset (not including cellulose, pinic acid, phthalic acid, and 3-MBTCA) and parameters similar to that in the SOURCES project (Weber et al., 2019) was performed, hereafter called "classic", and the results were compared with those from the present study (called "orga"). Figure 7 shows
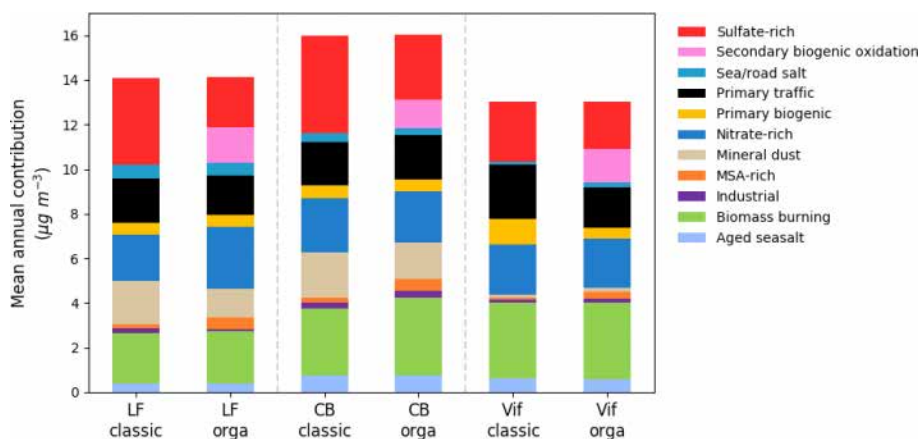
Figure 7. Mean annual contribution (μg m^{-3}) of PMF-resolved factors of PM$_{10}$ in the Grenoble basin using a classic set of input variables similar to SOURCES ("classic") and using additional new organic tracers ("orga").

the comparison of the yearly average mass contribution of the different factors for these two approaches. A detailed comparison of chemical profiles between the "classic" and "orga" PMF runs in each site is summarized in Sect. S3. One can see that most observations below are consistent in all three sites.

Some factors remain unaffected or only marginally modified: it is the case for the biomass burning source with a percentage increase in contribution, only ranging from 1 % to 14 %, in the "orga" compared to the "classic" PMF run across all sites. The primary biogenic source also posed an interesting case with a minimal decrease in contribution at 0.1 % and 6 % in the LF and CB sites, respectively. However, adding more specific biogenic tracers changed the contribution of the primary biogenic factor in Vif, from 1.1 μg m^{-3} for the "classic" PMF down to 0.50 μg m^{-3} for the "orga" PMF run, a value that is much more in line with the contributions observed at the other sites (0.56 and 0.55 μg m^{-3} in CB and LF, respectively). This further highlights the usefulness of the additional organic tracers (e.g., addition of cellulose in the primary biogenic factor), especially for specific site typologies.

Conversely, the most impacted factor is the sulfate-rich one, to a similar extent for the three sites with a much higher mass fraction in the "classic" PMF run in large part due to higher loadings of OC*. It may indicate possible merging with organic aerosol sources in the "classic" PMF, as presented in a comparison of chemical profiles between the "classic" and "orga" PMF runs in each site summarized in Sect. S3. Figure 7 shows that the differences are really close to the content of the new secondary biogenic oxidation factor. Secondary aerosols, such as the sulfate-rich factor, can be transported over long distances and can remain in the atmosphere for about a week (Warneck, 2000), allowing them to interact with numerous other species and undergo different atmospheric oxidation processes. In fact, several studies have investigated various oxidation pathways of sulfate-rich

sources (Barker et al., 2019; Ishizuka et al., 2000; Schneider et al., 2001; Ullerstam et al., 2002, 2003; Usher et al., 2002). In the SPECIEUROPE database, several studies have reported sulfate-rich sources influenced by a variety of different fuel combustion sources (Bove et al., 2014; Pernigotti et al., 2016; Pey et al., 2013). It is, therefore, not surprising that part of the matter in the sulfate-rich source was re-assigned to different other sources upon addition of the organic tracers in the "orga" PMF run. A comparable study in Metz (France) also used another organic tracer (oxalate) to apportion a secondary organic aerosol (SOA) source from PM, ascribing it possibly to both biogenic and anthropogenic emissions (Petit et al., 2019).

We also observed an increase in the contributions of the MSA-rich factor at the three sites, with an increase in contributions from specific inorganic species, such as SO$_4^{2-}$ and NH$_4^+$ (see Fig. S3.8.1). Conversely, a decrease in contribution from polyols was observed in the chemical profile of primary biogenic factor in Vif (see Fig. S3.7.1). Results show that in the "classic" PMF run, the contribution of polyols was almost completely assigned to the primary biogenic factor (> 94 % of its total mass). On the other hand, the "orga" PMF run resulted in a contribution of polyols to the MSA-rich factor of about 10 % of its total mass.

Finally, there is also an observed re-assignment of the Ca^{2+} species that further refined specific factors in Vif. The mineral dust factor is often identified with high loadings of Ca^{2+}; however, this is not the case for Vif, particularly for the "classic" PMF run (less than 1 % of total Ca^{2+}, although attached with important uncertainties). It is important to note that Ca^{2+} in an urban environment can come from several sources such as construction activities and global resuspended dust from various activities (from biomass burning and traffic). Previous studies comparing measurements at LF and a site close to a highway (2 km apart) showed a 34 % increment of this factor near the highway, supporting

the influence of resuspended dust with traffic (Charron et al., 2019). With the addition of the organic tracers, there was an observed increase in the contribution of Ca^{2+} in the mineral dust factor in Vif (see Fig. S3.11.1), resulting in more than 20 % of the total Ca^{2+} apportioned in this factor (a value is still attached with important uncertainties). Interestingly, the contribution of Ca^{2+} is mainly transferred from the primary traffic factor to the mineral dust factor. This resulted in a decreased contribution of the primary traffic factor in Vif from 2.4 µg m^{-3} for the "classic" PMF down to 1.8 µg m^{-3} for the "orga" PMF run. Again, this is a value closer to the contributions at the other sites (2.0 and 1.8 µg m^{-3} in CB and LF, respectively) (see Fig. S3.2.1).

3.3.3 Decrease in uncertainties

Another advantage of adding specific proxies in the PMF is the lowering of uncertainties associated with some other chemical species in some factors. Indeed, we observed a decrease in the BS uncertainties, notably for the OC* and also for some main tracers of sources in several profiles (see in the SI (S3)). The sulfate-rich is the most impacted factor when adding the new organic tracers and the higher uncertainties in the "classic" PMF run provided insights that this profile may have some internal mixing. Splitting this factor, thanks to the new organics, refined the sulfate-rich factor and strengthened the BS stability of this factor, decreasing the BS uncertainties.

Concerning the DISP, the range of uncertainties was also narrowed for 74 % of the species in factors when comparing the "classic" and "orga" PMF. This decrease in uncertainties for the DISP when adding new variables was already observed by (Emami and Hopke, 2017), but our study additionally observed this in the BS error estimation. Overall, on top of being able to identify new factors, the addition of the new specific proxies in the PMF strengthened the confidence we have for all other factors.

3.4 Fine-scale variability of the temporal contribution

Figure 3 indicates correlations of the concentrations for many chemical species across the sites. Additionally, the temporal evolution of the contribution of commonly resolved factors are further investigated in this section. Figure 8 presents the Pearson correlation coefficient of the contributions of the sources for the three pairs of sites. The sources that resulted in consistently strong correlations ($r > 0.77$) across all sites are biomass burning, nitrate-rich, aged sea salt, MSA-rich, secondary biogenic oxidation, and primary biogenic sources. The sea/road salt factor showed good correlations across the sites with a correlation coefficient ranging from 0.58 to 0.76.

Factors with strong seasonality appeared to be highly correlated between sites (biomass burning, nitrate-rich, MSA-rich, and primary biogenic). This tends to affirm that such factors are dominated either by large-scale transport (i.e.,

nitrate-rich) or by a strong climatic determinant. It is interesting to note that the primary biogenic factor presents systematically a slightly lower correlation than the polyols (LF-CB: $r_{\text{polyols}} = 0.94$ to $r_{\text{primary biogenic}} = 0.91$, LF-Vif: $r_{\text{polyols}} = 0.92$ to $r_{\text{primary biogenic}} = 0.88$ and Vif-CB: $r_{\text{polyols}} = 0.87$ to $r_{\text{primary biogenic}} = 0.82$). This may suggest a secondary process or a combination of several different primary processes in the primary biogenic factor affecting the sites at different rates (Petit et al., 2019; Samaké et al., 2019b). We also clearly see a stronger similarity between the two urban sites (LF and CB) compared to the peri urban one, notably for the primary traffic, mineral dust, and, to a lower extent, the industrial factor. This may be explained not only by the proximity of the location of the two former sites within the city, but also by their similarity in typology compared to the peri-urban site type in Vif. However, there are two factors that do not present good correlation between all sites.

One of them is the sulfate-rich factor which presents a similar contribution when comparing LF and Vif but low to no correlation when compared to CB. A deeper analysis shows that the sulfate-rich, together with the nitrate-rich factor in CB, explains a large part of the winter spike of secondary inorganics (23/24 Feburary 2018), whereas in LF and Vif only the nitrate-rich factor explains most of it. This spike drives the Pearson correlation coefficient to a low value and, without it, the correlation increases drastically (see Fig. S5.1 for the full scatterplot). Some PMF solutions of the BS in LF and Vif also had this behavior but were not chosen as the "best" solution. We propose two hypotheses for this difference: (1) during winter, some heterogeneous chemistry may take place in fog episodes in the Grenoble basin (resulting in episodic spikes in the SO$_4^{2-}$ contribution) that may not be spatially homogeneous at a city scale, leading to mixing of secondary sources, and (2) we have reached the limit of the PMF methodology to de-convolute further the secondary inorganics. Both hypotheses may be concurrent.

A further indication of a potential mixing between the sulfate- and nitrate-rich factors is presented in Fig. S5.3. In this figure, the total mass concentration of PM and major ions (SO$_4^{2-}$, NO$_3^-$, and NH$_4^+$) were compared between sites when the sulfate- and nitrate-rich factors were combined. Strong correlations between sites were found indicating similarity of such concentrations in secondary sources. It is out of scope of this work to determine whether this is a limitation of the PMF approach or whether there are some processes leading to real differences. We note however that apart from these spikes, the SO$_4^{2-}$ apportioned by this factor at three sites are in good agreement, and are within the uncertainties of each other (see Fig. 9). This figure also highlights that the uncertainty for the SO$_4^{2-}$ in this factor is higher for the CB site, as also shown in the chemical profile in Fig. S3.6.

The second factor which showed low correlations between pairs of sites is mineral dust, specifically when comparing Vif to the two other sites. This is in line with the difference in the PM$_{10}$ apportioned by this factor as shown in the previous sec-
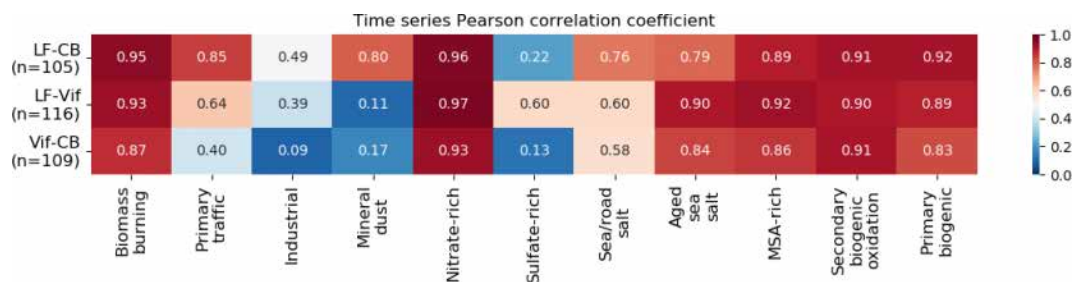
Figure 8. Heat map of the time series Pearson correlation coefficient of all factor contributions between LF and CB (LF-CB), LF and Vif (LF-Vif), and CB and Vif (CB-Vif).
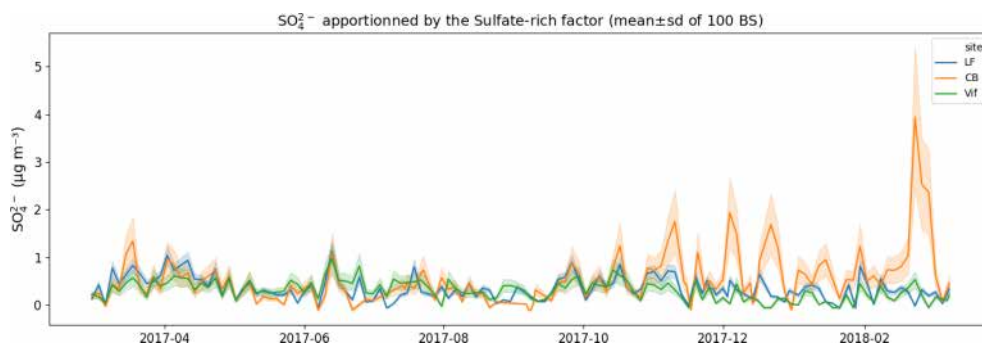

Figure 9. SO$_4^{2-}$ apportioned by the sulfate-rich factor at the three sites, according to the uncertainties given by the 100 BS as shown by the mean (solid line) and the standard deviation (shaded area).

tion. However, a closer look at the contribution scatterplot of Vif$_{Mineral\ dust}$ vs. CB$_{Mineral\ dust}$ (see Fig. S5.2) highlights that some events are very close to the 1 : 1 line. This is indicative of two regimes for mineral dust, with differences due to some specificity in the atmospheric dynamics in the valley near the surface. To investigate it further, a potential source contribution function (PSCF) analysis of the mineral dust factor for the Vif and CB sites was performed in order to assess the origin of air masses of this factor (Fig. 10). For the Vif site, the main origin is Spain, with well-defined air flow canalized by the valley and katabatic flows in a south-to-north direction (a phenomenon also reported in Largeron and Staquet, 2016). On the other hand, the origin for CB is not as well-defined. These PSCF pattern tends to indicate that the sources of the mineral dust factor present a strong local component for the urban sites (CB and LF being very similar), while the origin of the mineral dust factor in Vif appears to be mainly affected by long-range transport of dust only.

3.5 Fine-scale variability of chemical profiles

An additional similarity test was also performed to investigate the fine-scale variabilities of the chemical profiles of the factors. A similarity analysis at a regional scale in France identified stable chemical profiles obtained by PMF studies across many sites, corresponding to biomass burning, sulfate-rich, nitrate-rich, and fresh sea salt factors (Weber et

al., 2019). In our study, a parallel analysis was performed in order to evaluate the stability of the chemical profiles of the identified factors in high-proximity receptor locations. Briefly, PMF-resolved sources were compared for each pair of sites using both PD and SID to obtain a similarity metric (PD-SID).

3.5.1 (Dis-)similarity of the chemical profiles at the three sites

Figure 11 presents the similarity plot (PD-SID) obtained for the 11 factors found in this study. The biomass burning factor yielded the most stable chemical profile in all the sites in the Grenoble basin, which is consistent. Other stable factors include sulfate- and nitrate-rich, primary biogenic, MSA-rich, and secondary biogenic oxidation. The industrial and sea/road salt factors, both marginally above the accepted PD metric, could be considered as having heterogeneous profiles based on the contributions of these sources to the total PM$_{10}$ in each site.

However, a clear heterogeneous chemical profile was found in the mineral dust, this further emphasized the difference in origin of this factor as previously discussed in Sect. 3.4. More details about of the chemical profile of this factor can be found Fig. S3.11. One of the main differences is the lack of OC* in the Vif site compared to LF and CB sites, together with a much lower Ca^{2+} contribution. Additionally,
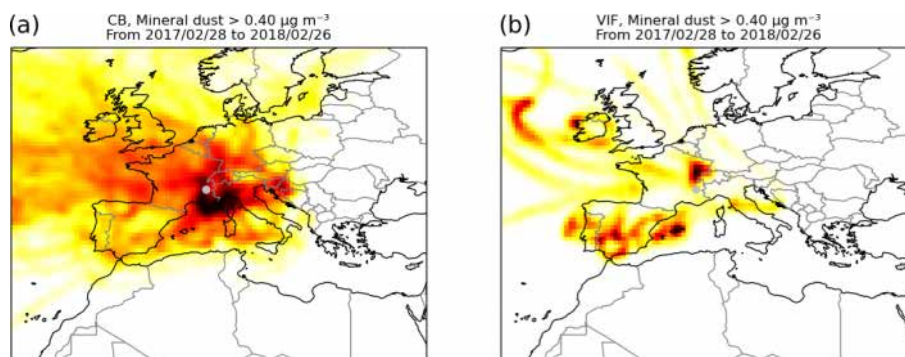
Figure 10. The PSCF analysis of the days with a mineral dust loading higher than $0.4\,\mu g\,m^{-3}$ for the CB site **(a)** and Vif **(b)**. Darker shades indicate higher probability density of source origin.
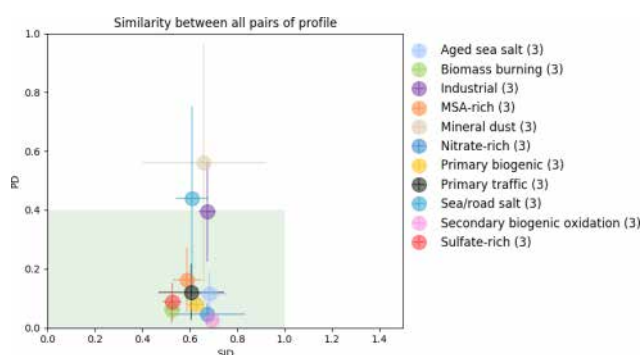

Figure 11. Similarity plot of all chemical profiles in each site. The shaded area (in green) shows the acceptable range of the PD-SID metric. For each point, the error bars represent the standard deviation of the three pairs of comparisons.

there is a lower SO$_4^{2-}$ apportioned in the mineral dust factor in Vif. The only similarity between all the sites are the high loadings of Al, Ti, and V as well as important contributions from other crustal metals (Fe, Ni, Mn). It also has to be noted that the cellulose is present up to about 20 % of its total mass in the mineral dust profile in the CB site; however, the BS estimates indicate very important uncertainties for this species in this factor (see Fig. S3.11).

Surprisingly, the sulfate-rich factor chemistry is one of the most stable profiles, although its temporal contributions exhibit high spatial variation, notably at CB compared to the LF and Vif sites.

Finally, although the primary traffic factor showed a stable profile based on the similarity plot (PD-SID metric), it has to be noted that, in the reference run (i.e., constrained), the species concentrations are within the BS uncertainties for all species at LF and CB sites but outside the BS range for the Vif site (see Fig. 12). Notably, the BS predicted higher contribution from Cu, Fe, Sb and Sn, which are common tracers of tyre and brake wear, than the reference run. Additionally, the Ca^{2+} is overestimated in the reference run by a large amount, as well as the OC*, and, to a lesser extent, the recon-

structed PM$_{10}$. Such BS results indicate that, in Vif, the primary traffic factor is heavily influenced by this phenomenon on specific days, which has led to an overestimation of the total PM$_{10}$ apportioned by this factor. Additionally, even at low concentrations, some terrestrial elements (Al, As, Ti) and cellulose are present in the primary traffic factor. As a result, even if the primary traffic characteristic of this factor is dominant, the influence of road dust re-suspension is not negligible for this factor in Vif.

3.5.2 Comparison with other chemical profiles of PM$_{10}$ sources from a regional study

It is interesting to evaluate whether a PMF study conducted at a city scale is leading to more similar source chemical profiles than a study using a database from a much larger area. Another question is whether PMF can produce more similar chemical source profiles with the help of additional organic tracers than a "classic" PMF run. Hence, the results obtained here are compared to those in the SOURCES program (Weber et al., 2019) for the nine factors common in both studies (the secondary biogenic factor was not identified in the SOURCES program with the data sets not including its proper chemical tracers). This can be represented with the projection on a similarity plot of the distances between the factors for the three pairs of sites over the Grenoble basin, both for the "classic" and "orga" PMF. This is compared to the results from all possible pairs of sites within the 15 sites of the SOURCES study (distributed over France), mapped with a probability density function of similarities. Figure 13 presents these plots for the factors "primary traffic" and "sulfate-rich", the other factors being presented in Sect. S6.

In most instances, the PMF results obtained for the Grenoble basin deliver slightly closer chemical profiles, both for the PD (sensitive to major components) and the SID (sensitive to the global profile), than the studies across more distant sites. This is particularly the case when comparing the two urban sites (LF and CB) (cf. Fig. 11). Some values out of
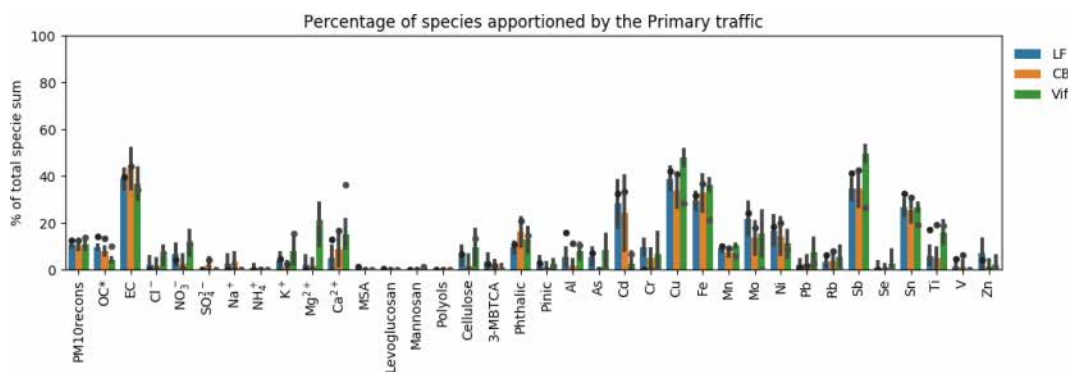
Figure 12. Percentage (%) of each species apportioned by the primary traffic factor (dots refer to the constrained run, bar plots refer to the mean, and error bars refer to the standard deviation of the 100 BS).
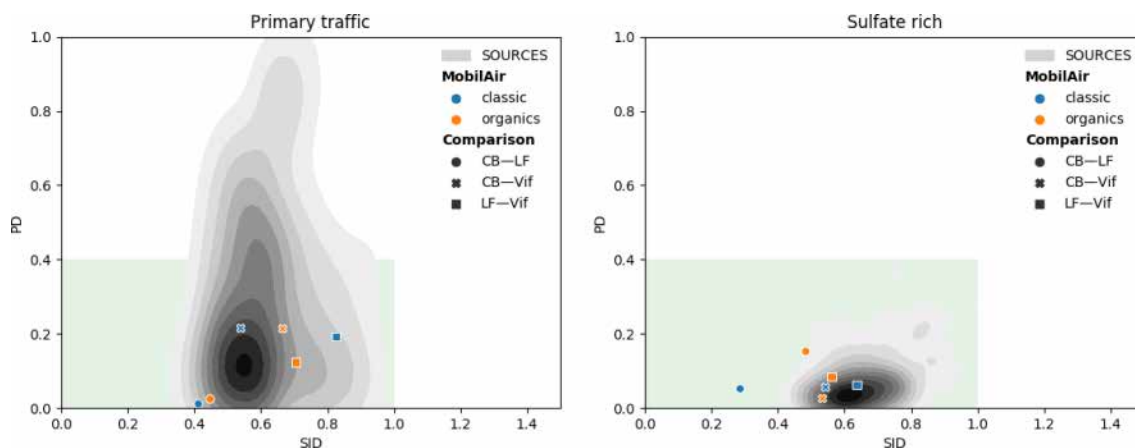

Figure 13. Similarity plots for the factors "primary traffic" and "sulfate-rich" for the pairs of sites formed in this study (Mobil'Air) compared to the probability density function of similarities obtained for the 15 French sites of the SOURCES program.

the acceptable range remain for some factors (mineral dust, industrial), involving the differences between the urban and suburban sites but are still fitting with the pattern obtained for the overall French sites. The addition of the organic tracers did not alter the source profiles of the commonly resolved PMF factors and, in fact, even enhanced it by further refining the other identified sources. This is predominantly seen in the MSA-rich factor, where some of the "classic" PMF results fell outside the acceptable range, while the "orga" PMFs are all in the acceptable range of the similarity plot. The "orga" PMF run for some factors such as primary biogenic, dust, and industrial factor also mostly yielded better PD and SID metrics (closer to the acceptable range) than the "classic" PMF run.

3.6 Improvement of the identified sources with the new organic tracers

In order to comprehensively apportion PM$_{10}$ sources, the very large unknown portion of OM, especially in the secondary fraction, needs to be properly identified. Most source

apportionment studies only use standard input variables including OC, EC, ions, and metals. However, these species alone are insufficient to describe the complexity of the organic matter, making it a challenge to apportion sources from the OM fraction and their formation processes (i.e., primary or secondary origin) (Srivastava et al., 2018a). Only a small number of studies have used organic tracers to apportion SOA in PM using PMF, and even these studies usually have limited number of samples, number of tracers, and/or identified sources (Feng et al., 2013; Shrivastava et al., 2007; Srivastava et al., 2018b). A few of these studies have proposed to estimate SOC contributions from the sum of OC loadings in the secondary inorganic (nitrate- and sulfate-rich) factor (Hu et al., 2010; Ke et al., 2008; Lee et al., 2008; Pachon et al., 2010; Yuan et al., 2006) or from water-soluble OC and humic-like substances (Qiao et al., 2018). Some have estimated the contributions of biogenic SOA from the oxidation products of isoprene, alpha-pinene, and beta-caryophyllene (Heo et al., 2013; Kleindienst et al., 2007; Miyazaki et al., 2012; Shrivastava et al., 2007; Wang et al., 2012). In fact, the high contributions of biogenic SOA during warmer peri-

ods, which could range from 20 % to 60 % (Heo et al., 2013; Miyazaki et al., 2012; Wang et al., 2012; Zhang et al., 2010), found by other PMF studies is also consistent with our findings. Wang et al. (2017a) also highlighted the importance of biogenic SOA tracers as it significantly impacts the source apportionment results, particularly in areas with strong SOA contributions. Although applied to a small sample size, an interesting technique assimilating polar SOA tracers and primary organic aerosol (POA) tracers was performed by Hu et al. (2010). This resulted in two identified SOA factors that are mixed with (1) secondary inorganics and biomass burning and (2) green waste and biomass burning. Hence, with the appropriate uncertainties, the SOA tracers can be a practical way, possibly even necessary, of estimating SOA contributions (Feng et al., 2013), especially in urban areas (Wang et al., 2012).

Our study demonstrated that the use of organic tracers aided an effective source-specific approach that clearly identified major sources of SOA in PM$_{10}$ such as MSA-rich and secondary biogenic oxidation sources. The potential influence of anthropogenic emissions on some sources was also observed through the contribution of one of the organic tracers used, phthalic acid. The sufficient number of samples ($n > 125$ for each site) in our study have also maintained the statistical robustness of the solutions obtained from filter-based measurements. The stability of the organic tracers also resulted in homogeneous chemical profiles which allowed seamless identification of uncommonly resolved sources such as primary biogenic, secondary biogenic oxidation, and MSA-rich. Although the addition of cellulose did not emerge as a separate biogenic factor, it provided an option to scrutinize the difference in terms origin of the primary biogenic sources across sites. Overall, the organic tracers have further refined the contribution of other identified sources by taking in consideration the SOA portion of PM$_{10}$ that would have otherwise mixed with other sources and have facilitated an innovative approach to improve the apportionment of PM$_{10}$ sources.

4   Conclusions

A fine-scale source apportionment of PM$_{10}$ in different urban typologies (background, pedestrianized hyper-center, and peri-urban) in a small-scale area (< 15 km) was performed using PMF 5.0. Additional organic tracers (MSA, cellulose, 3-MBTCA, pinic acid, and phthalic acid) were used to supplement the standard input variables. An 11-factor optimal solution was found for each of the three urban sites, including primary traffic, nitrate-rich, sulfate-rich, industrial, biomass burning, aged sea salt, sea/road salt, mineral dust, primary biogenic, secondary biogenic oxidation, and MSA-rich sources. The results from previously reported PMF studies in Grenoble (Srivastava et al., 2018b; Weber et al., 2019) were confirmed by the findings in this study particularly

the long-term stability of regional source emissions 5 years apart. The PMF solution obtained with the additional organic tracers resulted in

1. the improvement of PM$_{10}$ mass closure and the exploration of appropriate input variable uncertainties;

2. the re-assignment of the bulk sulfate-rich factor contribution to more descriptive secondary aerosol sources in the atmosphere;

3. the clear identification of commonly unresolved sources in the SOA fraction (e.g., primary biogenic, traced by the polyols and cellulose; secondary biogenic oxidation, traced by 3-MBTCA and pinic acid; and MSA-rich, traced by the MSA) in different urban typologies;

4. the decreased uncertainties, for both BS and DISP error estimates, that further strengthened confidence in the PMF solution; and

5. the increased knowledge of the stability of the chemical profiles of the factors, which could be a key when using them in further large-scale analysis or modeling.

The three-site comparison at a local scale

6. highlights very similar profiles and temporal evolution in the factor contributions at a conurbation scale (such as the Grenoble basin);

7. allows the determination of local heterogeneities in a small-scale area; and

8. pointed out some difficulties to disentangle the secondary inorganic sources (NO$_3^-$ and SO$_4^{2-}$) and some mixing between both species may occur.

Overall, an enhanced and fine-scale source profile of PM$_{10}$ was obtained in the Grenoble basin. The trend observed in the MSA-rich, secondary biogenic oxidation, and primary biogenic factors showed the extent of this phenomenon suggesting importance of the contribution of biogenic sources, both primary and secondary. The significant percentage attributed to SOA sources revealed the strong necessity of organic molecular tracers in fully discriminating the origins of PM$_{10}$ sources.

References

Alleman, L. Y., Lamaison, L., Perdrix, E., Robache, A., and Galloo, J.-C.: PM$_{10}$ metal concentrations and source identification using positive matrix factorization and wind sectoring in a French industrial zone, Atmos. Res., 96, 612–625, https://doi.org/10.1016/j.atmosres.2010.02.008, 2010.

Atkinson, R. and Arey, J.: Atmospheric Chemistry of Biogenic Organic Compounds, Accounts Chem. Res., 31, 574–583, https://doi.org/10.1021/ar970143z, 1998.

Aymoz, G., Jaffrezo, J. L., Chapuis, D., Cozic, J., and Maenhaut, W.: Seasonal variation of PM$_{10}$ main constituents in two valleys of the French Alps. I: EC/OC fractions, Atmos. Chem. Phys., 7, 661–675, https://doi.org/10.5194/acp-7-661-2007, 2007.

Ayres, J. G., Borm, P., Cassee, F. R., Castranova, V., Donaldson, K., Ghio, A., Harrison, R. M., Hider, R., Kelly, F., Kooter, I. M., Marano, F., Maynard, R. L., Mudway, I., Nel, A., Sioutas, C., Smith, S., Baeza-Squiban, A., Cho, A., Duggan, S., and Froines, J.: Evaluating the Toxicity of Airborne Particulate Matter and Nanoparticles by Measuring Oxidative Stress Potential – A Workshop Report and Consensus Statement, Inhal. Toxicol., 20, 75–99, https://doi.org/10.1080/08958370701665517, 2008.

Barker, J. R., Steiner, A. L., and Wallington, T. J.: Advances in Atmospheric Chemistry: Volume 2: Organic Oxidation and Multiphase Chemistry, World Scientific, Singapore, 2019.

Bauer, H., Kasper-Giebl, A., Löflund, M., Giebl, H., Hitzenberger, R., Zibuschka, F., and Puxbaum, H.: The contribution of bacteria and fungal spores to the organic carbon content of cloud water, precipitation and aerosols, Atmos. Res., 64, 109–119, https://doi.org/10.1016/S0169-8095(02)00084-4, 2002.

Belis, C. A., Favez, O., Harrison, R. M., Larsen, B. R., Amato, F., El Haddad, I., Hopke, P. K., Nava, S., Paatero, P., Prévôt, A., Quass, U., Vecchi, R., and Viana, M.: European Commission, Joint Research Centre, and Institute for Environment and Sustainability: European guide on air pollution source apportionment with receptor models, Publications Office, Luxembourg, 2014.

Belis, C. A., Pernigotti, D., Karagulian, F., Pirovano, G., Larsen, B. R., Gerboles, M., and Hopke, P. K.: A new methodology to assess the performance and uncertainty of source apportionment models in intercomparison exercises, Atmos. Environ., 119, 35–44, https://doi.org/10.1016/j.atmosenv.2015.08.002, 2015.

Belis, C. A., Pikridas, M., Lucarelli, F., Petralia, E., Cavalli, F., Calzolai, G., Berico, M., and Sciare, J.: Source apportionment of fine PM by combining high time resolution organic and inorganic chemical composition datasets, Atmos. Environ. X, 3, 100046, https://doi.org/10.1016/j.aeaoa.2019.100046, 2019.

Belis, C. A., Pernigotti, D., Pirovano, G., Favez, O., Jaffrezo, J. L., Kuenen, J., Denier van Der Gon, H., Reizer, M., Riffault, V., Alleman, L. Y., Almeida, M., Amato, F., Angyal, A., Argyropoulos, G., Bande, S., Beslic, I., Besombes, J.-L., Bove, M. C., Brotto, P., Calori, G., Cesari, D., Colombi, C., Contini, D., De Gennaro, G., Di Gilio, A., Diapouli, E., El Haddad, I., Elbern, H., Eleftheriadis, K., Ferreira, J., Vivanco, M. G., Gilardoni, S., Golly, B., Hellebust, S., Hopke, P. K., Izadmanesh, Y., Jorquera, H., Krajsek, K., Kranenburg, R., Lazzeri, P., Lenartz, F., Lucarelli, F., Maciejewska, K., Manders, A., Manousakas, M., Masiol, M., Mircea, M., Mooibroek, D., Nava, S., Oliveira, D., Paglione, M., Pandolfi, M., Perrone, M., Petralia, E., Pietrodangelo, A., Pillon, S., Pokorna, P., Prati, P., Salameh, D., Samara, C., Samek, L., Saraga, D., Sauvage, S., Schaap, M., Scotto, F., Sega, K., Siour, G., Tauler, R., Valli, G., Vecchi, R., Venturini, E., Vestenius, M., Waked, A., and Yubero, E.: Evaluation of receptor and chemical transport models for PM$_{10}$ source apportionment, Atmos. Environ. X, 5, 100053, https://doi.org/10.1016/j.aeaoa.2019.100053, 2020.

Bessagnet, B., Menut, L., Lapere, R., Couvidat, F., Jaffrezo, J.-L., Mailler, S., Favez, O., Pennel, R., and Siour, G.: High Resolution Chemistry Transport Modeling with the On-Line CHIMERE-WRF Model over the French Alps – Analysis of a Feedback of Surface Particulate Matter Concentrations on Mountain Meteorology, Atmosphere, 11, 565, https://doi.org/10.3390/atmos11060565, 2020.

Birch, M. E. and Cary, R. A.: Elemental Carbon-Based Method for Monitoring Occupational Exposures to Particulate Diesel Exhaust, Aerosol Sci. Tech., 25, 221–241, https://doi.org/10.1080/02786829608965393, 1996.

Borlaza, L. J. S., Weber, S., Jaffrezo, J.-L., Houdier, S., Slama, R., Rieux, C., Albinet, A., Micallef, S., Trébluchon, C., and Uzu, G.: Disparities in particulate matter (PM$_{10}$) origins and oxidative potential at a city-scale (Grenoble, France) – Part II: Sources of PM$_{10}$ oxidative potential using multiple linear regression analysis and the predictive applicability of multilayer perceptron neural network analysis, Atmos. Chem. Phys. Discuss. [preprint], https://doi.org/10.5194/acp-2021-57, in review, 2021.

Bove, M. C., Brotto, P., Cassola, F., Cuccia, E., Massabò, D., Mazzino, A., Piazzalunga, A., and Prati, P.: An integrated PM$_{2.5}$ source apportionment study: Positive Matrix Factorisation vs. the chemical transport model CAMx, Atmos. Environ., 94, 274–286, https://doi.org/10.1016/j.atmosenv.2014.05.039, 2014.

Bozzetti, C., Daellenbach, K. R., Hueglin, C., Fermo, P., Sciare, J., Kasper-Giebl, A., Mazar, Y., Abbaszade, G., El Kazzi, M., Gonzalez, R., Shuster-Meiseles, T., Flasch, M., Wolf, R., Křepelová, A., Canonaco, F., Schnelle-Kreis, J., Slowik, J. G., Zimmermann, R., Rudich, Y., Baltensperger, U., El Haddad, I., and Prévôt, A. S. H.: Size-Resolved Identification, Characterization, and Quantification of Primary Biological Organic Aerosol at a European Rural Site, Environ. Sci. Technol., 50, 3425–3434, https://doi.org/10.1021/acs.est.5b05960, 2016.

Bozzetti, C., Sosedova, Y., Xiao, M., Daellenbach, K. R., Ulevicius, V., Dudoitis, V., Mordas, G., Byčenkienė, S., Plauškaitė, K., Vlachou, A., Golly, B., Chazeau, B., Besombes, J.-L., Baltensperger, U., Jaffrezo, J.-L., Slowik, J. G., El Haddad, I., and Prévôt, A. S. H.: Argon offline-AMS source apportionment of organic aerosol over yearly cycles for an urban, rural, and marine site in northern Europe, Atmos. Chem. Phys., 17, 117–141, https://doi.org/10.5194/acp-17-117-2017, 2017.

Brunekreef, B.: Epidemiological evidence of effects of coarse airborne particles on health, Eur. Respir. J., 26, 309–318, https://doi.org/10.1183/09031936.05.00001805, 2005.

Budisulistiorini, S. H., Canagaratna, M. R., Croteau, P. L., Marth, W. J., Baumann, K., Edgerton, E. S., Shaw, S. L., Knipping, E. M., Worsnop, D. R., Jayne, J. T., Gold, A., and Surratt, J. D.: Real-Time Continuous Characterization of Secondary Organic Aerosol Derived from Isoprene Epoxydiols in Downtown Atlanta, Georgia, Using the Aerodyne Aerosol Chemical Speciation Monitor, Environ. Sci. Technol., 47, 5686–5694, https://doi.org/10.1021/es400023n, 2013.

Budisulistiorini, S. H., Baumann, K., Edgerton, E. S., Bairai, S. T., Mueller, S., Shaw, S. L., Knipping, E. M., Gold, A., and Surratt, J. D.: Seasonal characterization of submicron aerosol chemical composition and organic aerosol sources in the southeastern United States: Atlanta, Georgia, and Look Rock, Tennessee, Atmos. Chem. Phys., 16, 5171–5189, https://doi.org/10.5194/acp-16-5171-2016, 2016.

Bullock, K. R., Duvall, R. M., Norris, G. A., McDow, S. R., and Hays, M. D.: Evaluation of the CMB and PMF models using organic molecular markers in fine particulate matter collected during the Pittsburgh Air Quality Study, Atmos. Environ., 42, 6897–6904, https://doi.org/10.1016/j.atmosenv.2008.05.011, 2008.

Cavalli, F., Viana, M., Yttri, K. E., Genberg, J., and Putaud, J.-P.: Toward a standardised thermal-optical protocol for measuring atmospheric organic and elemental carbon: the EUSAAR protocol, Atmos. Meas. Tech., 3, 79–89, https://doi.org/10.5194/amt-3-79-2010, 2010.

Charron, A., Polo-Rehn, L., Besombes, J.-L., Golly, B., Buisson, C., Chanut, H., Marchand, N., Guillaud, G., and Jaffrezo, J.-L.: Identification and quantification of particulate tracers of exhaust and non-exhaust vehicle emissions, Atmos. Chem. Phys., 19, 5187–5207, https://doi.org/10.5194/acp-19-5187-2019, 2019.

Chen, Q., Sherwen, T., Evans, M., and Alexander, B.: DMS oxidation and sulfur aerosol formation in the marine troposphere: a focus on reactive halogen and multiphase chemistry, Atmos. Chem. Phys., 18, 13617–13637, https://doi.org/10.5194/acp-18-13617-2018, 2018.

Chevrier, F.: Chauffage au bois et qualité de l'air en Vallée de l'Arve: définition d'un système de surveillance et impact d'une politique de rénovation du parc des appareils anciens., PhD Thesis, Université Grenoble Alpes, Grenoble, https://tel.archives-ouvertes.fr/tel-01527559 (last access: 28 June 2018), 2016.

Colette, A., Menut, L., Haeffelin, M., and Morille, Y.: Impact of the transport of aerosols from the free troposphere towards the boundary layer on the air quality in the Paris area, Atmos. Environ., 42, 390–402, https://doi.org/10.1016/j.atmosenv.2007.09.044, 2008.

Daellenbach, K. R., Kourtchev, I., Vogel, A. L., Bruns, E. A., Jiang, J., Petäjä, T., Jaffrezo, J.-L., Aksoyoglu, S., Kalberer, M., Baltensperger, U., El Haddad, I., and Prévôt, A. S. H.: Impact of anthropogenic and biogenic sources on the seasonal variation in the molecular composition of urban organic aerosols: a field and laboratory study using ultra-high-resolution mass spectrometry, Atmos. Chem. Phys., 19, 5973–5991, https://doi.org/10.5194/acp-19-5973-2019, 2019.

Dai, Q., Liu, B., Bi, X., Wu, J., Liang, D., Zhang, Y., Feng, Y., and Hopke, P. K.: Dispersion Normalized PMF Provides Insights into the Significant Changes in Source Contributions to PM$_{2.5}$ after the COVID-19 Outbreak, Environ. Sci. Technol., 54, acs.est.0c02776, https://doi.org/10.1021/acs.est.0c02776, 2020a.

Dai, Q., Hopke, P. K., Bi, X., and Feng, Y.: Improving apportionment of PM$_{2.5}$ using multisite PMF by constraining G-values with a prioriinformation, Sci. Total Environ., 736, 139657, https://doi.org/10.1016/j.scitotenv.2020.139657, 2020b.

Emami, F. and Hopke, P. K.: Effect of adding variables on rotational ambiguity in positive matrix factorization solutions, Chemometr. Intell. Lab., 162, 198–202, https://doi.org/10.1016/j.chemolab.2017.01.012, 2017.

Favez, O., El Haddad, I., Piot, C., Boréave, A., Abidi, E., Marchand, N., Jaffrezo, J.-L., Besombes, J.-L., Personnaz, M.-B., Sciare, J., Wortham, H., George, C., and D'Anna, B.: Intercomparison of source apportionment models for the estimation of wood burning aerosols during wintertime in an Alpine city (Grenoble, France), Atmos. Chem. Phys., 10, 5295–5314, https://doi.org/10.5194/acp-10-5295-2010, 2010.

Favez, O., Weber, S., Petit, J.-E., Alleman, L. Y., Albinet, A., Riffault, V., Chazeau, B., Amodeo, T., Salameh, D., Zhang, Y., Srivastava, D., Samaké, A., Aujay-Plouzeau, R., Papin, A., Bonnaire, N., Boullanger, C., Chatain, M., Chevrier, F., Detournay, A., Dominik-Sègue, M., Falhun, R., Garbin, C., Ghersi, V., Grignion, G., Levigoureux, G., Pontet, S., Rangognio, J., Zhang, S., Besombes, J.-L., Conil, S., Uzu, G., Savarino, J., Marchand, N., Gros, V., Marchand, C., Jaffrezo, J.-L., and Leoz-Garziandia, E.: Overview of the French Operational Network for In Situ Observation of PM Chemical Composition and Sources

in Urban Environments (CARA Program), Atmosphere, 12, 207, https://doi.org/10.3390/atmos12020207, 2021.

Feng, J., Li, M., Zhang, P., Gong, S., Zhong, M., Wu, M., Zheng, M., Chen, C., Wang, H., and Lou, S.: Investigation of the sources and seasonal variations of secondary organic aerosols in PM$_{2.5}$ in Shanghai with organic tracers, Atmos. Environ., 79, 614–622, https://doi.org/10.1016/j.atmosenv.2013.07.022, 2013.

Franchini, M. and Mannucci, P.: Particulate Air Pollution and Cardiovascular Risk: Short-term and Long-term Effects, Semin. Thromb. Hemost., 35, 665–670, https://doi.org/10.1055/s-0029-1242720, 2009.

Gelencsér, A., May, B., Simpson, D., Sánchez-Ochoa, A., Kasper-Giebl, A., Puxbaum, H., Caseiro, A., Pio, C., and Legrand, M.: Source apportionment of PM$_{2.5}$ organic aerosol over Europe: Primary/secondary, natural/anthropogenic, and fossil/biogenic origin, J. Geophys. Res., 112, D23S04, https://doi.org/10.1029/2006JD008094, 2007.

Gianini, M. F. D., Fischer, A., Gehrig, R., Ulrich, A., Wichser, A., Piot, C., Besombes, J.-L., and Hueglin, C.: Comparative source apportionment of PM$_{10}$ in Switzerland for 2008/2009 and 1998/1999 by Positive Matrix Factorisation, Atmos. Environ., 54, 149–158, https://doi.org/10.1016/j.atmosenv.2012.02.036, 2012.

Golly, B., Waked, A., Weber, S., Samake, A., Jacob, V., Conil, S., Rangognio, J., Chrétien, E., Vagnot, M.-P., Robic, P.-Y., Besombes, J.-L., and Jaffrezo, J.-L.: Organic markers and OC source apportionment for seasonal variations of PM$_{2.5}$ at 5 rural sites in France, Atmos. Environ., 198, 142–157, https://doi.org/10.1016/j.atmosenv.2018.10.027, 2019.

Graham, B., Guyon, P., Taylor, P. E., Artaxo, P., Maenhaut, W., Glovsky, M. M., Flagan, R. C., and Andreae, M. O.: Organic compounds present in the natural Amazonian aerosol: Characterization by gas chromatography-mass spectrometry: ORGANIC COMPOUNDS IN AMAZONIAN AEROSOLS, J. Geophys. Res., 108, 4766, https://doi.org/10.1029/2003JD003990, 2003.

Grover, B. D.: Measurement of total PM$_{2.5}$ mass (nonvolatile plus semivolatile) with the Filter Dynamic Measurement System tapered element oscillating microbalance monitor, J. Geophys. Res., 110, D07S03, https://doi.org/10.1029/2004JD004995, 2005.

Heo, J., Dulger, M., Olson, M. R., McGinnis, J. E., Shelton, B. R., Matsunaga, A., Sioutas, C., and Schauer, J. J.: Source apportionments of PM$_{2.5}$ organic carbon using molecular marker Positive Matrix Factorization and comparison of results from different receptor models, Atmos. Environ., 73, 51–61, https://doi.org/10.1016/j.atmosenv.2013.03.004, 2013.

Hopke, P. K.: Review of receptor modeling methods for source apportionment, JAPCA J. Air. Waste Ma., 66, 237–259, https://doi.org/10.1080/10962247.2016.1140693, 2016.

Horne, J. R. and Dabdub, D.: Impact of global climate change on ozone, particulate matter, and secondary organic aerosol concentrations in California: A model perturbation analysis, Atmos. Environ., 153, 1–17, https://doi.org/10.1016/j.atmosenv.2016.12.049, 2017.

Hu, D., Bian, Q., Lau, A. K. H., and Yu, J. Z.: Source apportioning of primary and secondary organic carbon in summer PM$_{2.5}$ in Hong Kong using positive matrix factorization of secondary and primary organic tracer data, J. Geophys. Res., 115, D16204, https://doi.org/10.1029/2009JD012498, 2010.

Hyder, M., Genberg, J., Sandahl, M., Swietlicki, E., and Jönsson, J. Å.: Yearly trend of dicarboxylic acids in organic aerosols from south of Sweden and source attribution, Atmos. Environ., 57, 197–204, https://doi.org/10.1016/j.atmosenv.2012.04.027, 2012.

Igarashi, Y., Kita, K., Maki, T., Kinase, T., Hayashi, N., Hosaka, K., Adachi, K., Kajino, M., Ishizuka, M., Sekiyama, T. T., Zaizen, Y., Takenaka, C., Ninomiya, K., Okochi, H., and Sorimachi, A.: Fungal spore involvement in the resuspension of radiocaesium in summer, Sci. Rep., 9, 1954, https://doi.org/10.1038/s41598-018-37698-x, 2019

Ishizuka, T., Kabashima, H., Yamaguchi, T., Tanabe, K., and Hattori, H.: Initial Step of Flue Gas DesulfurizationAn IR Study of the Reaction of SO$_2$ with NO$_x$ on CaO$^-$, Environ. Sci. Technol., 34, 2799–2803, https://doi.org/10.1021/es991073p, 2000.

Jaffrezo, J. L., Calas, N., and Bouchet, M.: Carboxylic acids measurements with ionic chromatography, Atmos. Environ., 32, 2705–2708, 1998.

Jardine, K., Yañez-Serrano, A. M., Williams, J., Kunert, N., Jardine, A., Taylor, T., Abrell, L., Artaxo, P., Guenther, A., Hewitt, C. N., House, E., Florentino, A. P., Manzi, A., Higuchi, N., Kesselmeier, J., Behrendt, T., Veres, P. R., Derstroff, B., Fuentes, J. D., Martin, S. T., and Andreae, M. O.: Dimethyl sulfide in the Amazon rain forest: DMS in the Amazon, Global Biogeochem. Cy., 29, 19–32, https://doi.org/10.1002/2014GB004969, 2015.

Jin, X., Xue, B., Zhou, Q., Su, R., and Li, Z.: Mitochondrial damage mediated by ROS incurs bronchial epithelial cell apoptosis upon ambient PM$_{2.5}$ exposure, J. Toxicol. Sci., 43, 101–111, https://doi.org/10.2131/jts.43.101, 2018.

Ke, L., Liu, W., Wang, Y., Russell, A. G., Edgerton, E. S., and Zheng, M.: Comparison of PM$_{2.5}$ source apportionment using positive matrix factorization and molecular marker-based chemical mass balance, Sci. Total Environ., 394, 290–302, https://doi.org/10.1016/j.scitotenv.2008.01.030, 2008.

Kleindienst, T. E., Jaoui, M., Lewandowski, M., Offenberg, J. H., Lewis, C. W., Bhave, P. V., and Edney, E. O.: Estimates of the contributions of biogenic and anthropogenic hydrocarbons to secondary organic aerosol at a southeastern US location, Atmos. Environ., 41, 8288–8300, https://doi.org/10.1016/j.atmosenv.2007.06.045, 2007.

Kunit, M. and Puxbaum, H.: Enzymatic determination of the cellulose content of atmospheric aerosols, Atmos. Environ., 30, 1233–1236, https://doi.org/10.1016/1352-2310(95)00429-7, 1996.

Langrish, J. P., Bosson, J., Unosson, J., Muala, A., Newby, D. E., Mills, N. L., Blomberg, A., and Sandström, T.: Cardiovascular effects of particulate air pollution exposure: time course and underlying mechanisms, J. Intern. Med., 272, 224–239, https://doi.org/10.1111/j.1365-2796.2012.02566.x, 2012.

Largeron, Y. and Staquet, C.: The Atmospheric Boundary Layer during Wintertime Persistent Inversions in the Grenoble Valleys, Front. Earth Sci., 4, 70, https://doi.org/10.3389/feart.2016.00070, 2016.

Lee, S., Liu, W., Wang, Y., Russell, A. G., and Edgerton, E. S.: Source apportionment of PM$_{2.5}$: Comparing PMF and CMB results for four ambient monitoring sites in the southeastern United States, Atmos. Environ., 42, 4126–4137, https://doi.org/10.1016/j.atmosenv.2008.01.025, 2008.

Li, S.-M., Barrie, L. A., Talbot, R. W., Harriss, R. C., Davidson, C. I., and Jaffrezo, J.-L.: Seasonal and geographic variations of methanesulfonic acid in the arctic troposphere, Atmos.

Environ. A-Gen., 27, 3011–3024, https://doi.org/10.1016/0960-1686(93)90333-T, 1993.

Marmur, A., Mulholland, J. A., and Russell, A. G.: Optimized variable source-profile approach for source apportionment, Atmos. Environ., 41, 493–505, https://doi.org/10.1016/j.atmosenv.2006.08.028, 2007.

McNeill, V. F.: Atmospheric Aerosols: Clouds, Chemistry, and Climate, Annu. Rev. Chem. Biomol., 8, 427–444, https://doi.org/10.1146/annurev-chembioeng-060816-101538, 2017.

Miyazaki, Y., Fu, P. Q., Kawamura, K., Mizoguchi, Y., and Yamanoi, K.: Seasonal variations of stable carbon isotopic composition and biogenic tracer compounds of water-soluble organic aerosols in a deciduous forest, Atmos. Chem. Phys., 12, 1367–1376, https://doi.org/10.5194/acp-12-1367-2012, 2012.

Nel, A.: ATMOSPHERE: Enhanced: Air Pollution-Related Illness: Effects of Particles, Science, 308, 804–806, https://doi.org/10.1126/science.1108752, 2005.

Norris, G., Duvall, R., Brown, S., and Bai, S.: Positive Matrix Factorization (PMF) 5.0 Fundamentals and User Guide, US Environmental Protection Agency, Office of Research and Development, Washington, D.C., 136 pp., 2014.

Ostro, B., Tobias, A., Querol, X., Alastuey, A., Amato, F., Pey, J., Pérez, N., and Sunyer, J.: The Effects of Particulate Matter Sources on Daily Mortality: A Case-Crossover Study of Barcelona, Spain, Environ. Health Persp., 119, 1781–1787, https://doi.org/10.1289/ehp.1103618, 2011.

Paatero, P.: The Multilinear Engine – A Table-Driven, Least Squares Program for Solving Multilinear Problems, Including the n-Way Parallel Factor Analysis Model, J. Comput. Graph. Stat., 8, 854–888, https://doi.org/10.1080/10618600.1999.10474853, 1999.

Paatero, P. and Tapper, U.: Positive matrix factorization: A non-negative factor model with optimal utilization of error estimates of data values, Environmetrics, 5, 111–126, https://doi.org/10.1002/env.3170050203, 1994.

Pachon, J. E., Balachandran, S., Hu, Y., Weber, R. J., Mulholland, J. A., and Russell, A. G.: Comparison of SOC estimates and uncertainties from aerosol chemical composition and gas phase data in Atlanta, Atmos. Environ., 44, 3907–3914, https://doi.org/10.1016/j.atmosenv.2010.07.017, 2010.

Pandolfi, M., Mooibroek, D., Hopke, P., van Pinxteren, D., Querol, X., Herrmann, H., Alastuey, A., Favez, O., Hüglin, C., Perdrix, E., Riffault, V., Sauvage, S., van der Swaluw, E., Tarasova, O., and Colette, A.: Long-range and local air pollution: what can we learn from chemical speciation of particulate matter at paired sites?, Atmos. Chem. Phys., 20, 409–429, https://doi.org/10.5194/acp-20-409-2020, 2020.

Pernigotti, D. and Belis, C. A.: DeltaSA tool for source apportionment benchmarking, description and sensitivity analysis, Atmos. Environ., 180, 138–148, https://doi.org/10.1016/j.atmosenv.2018.02.046, 2018.

Pernigotti, D., Belis, C. A., and Spanò, L.: SPECIEUROPE: The European data base for PM source profiles, Atmos. Pollut. Res., 7, 307–314, https://doi.org/10.1016/j.apr.2015.10.007, 2016.

Petit, J.-E., Pallarès, C., Favez, O., Alleman, L. Y., Bonnaire, N., and Rivière, E.: Sources and Geographical Origins of PM$_{10}$ in Metz (France) Using Oxalate as a Marker of Secondary Organic

Aerosols by Positive Matrix Factorization Analysis, Atmosphere, 10, 370, https://doi.org/10.3390/atmos10070370, 2019.

Pey, J., Alastuey, A., and Querol, X.: PM$_{10}$ and PM$_{2.5}$ sources at an insular location in the western Mediterranean by using source apportionment techniques, Sci. Total Environ., 456–457, 267–277, https://doi.org/10.1016/j.scitotenv.2013.03.084, 2013.

Piao, M. J., Ahn, M. J., Kang, K. A., Ryu, Y. S., Hyun, Y. J., Shilnikova, K., Zhen, A. X., Jeong, J. W., Choi, Y. H., Kang, H. K., Koh, Y. S., and Hyun, J. W.: Particulate matter 2.5 damages skin cells by inducing oxidative stress, subcellular organelle dysfunction, and apoptosis, Arch. Toxicol., 92, 2077–2091, https://doi.org/10.1007/s00204-018-2197-9, 2018.

Pindado, O. and Perez, R. M.: Source apportionment of particulate organic compounds in a rural area of Spain by positive matrix factorization, Atmos. Pollut. Res., 2, 492–505, https://doi.org/10.5094/APR.2011.056, 2011.

Putaud, J.-P., Van Dingenen, R., Alastuey, A., Bauer, H., Birmili, W., Cyrys, J., Flentje, H., Fuzzi, S., Gehrig, R., Hansson, H. C., Harrison, R. M., Herrmann, H., Hitzenberger, R., Hüglin, C., Jones, A. M., Kasper-Giebl, A., Kiss, G., Kousa, A., Kuhlbusch, T. A. J., Löschau, G., Maenhaut, W., Molnar, A., Moreno, T., Pekkanen, J., Perrino, C., Pitz, M., Puxbaum, H., Querol, X., Rodriguez, S., Salma, I., Schwarz, J., Smolik, J., Schneider, J., Spindler, G., ten Brink, H., Tursic, J., Viana, M., Wiedensohler, A., and Raes, F.: A European aerosol phenomenology – 3: Physical and chemical characteristics of particulate matter from 60 rural, urban, and kerbside sites across Europe, Atmos. Environ., 44, 1308–1320, https://doi.org/10.1016/j.atmosenv.2009.12.011, 2010.

Puxbaum, H.: Size distribution and seasonal variation of atmospheric cellulose, Atmos. Environ., 37, 3693–3699, https://doi.org/10.1016/S1352-2310(03)00451-5, 2003.

Qiao, F., Li, Q., and Lei, Y.: Particulate Matter Caused Health Risk in an Urban Area of the Middle East and the Challenges in Reducing its Anthropogenic Emissions, Environ. Pollut. Clim. Change, 2, 145, https://doi.org/10.4172/2573-458X.1000145, 2018.

Saeaw, N. and Thepanondh, S.: Source apportionment analysis of airborne VOCs using positive matrix factorization in industrial and urban areas in Thailand, Atmos. Pollut. Res., 6, 644–650, https://doi.org/10.5094/APR.2015.073, 2015.

Samaké, A., Jaffrezo, J.-L., Favez, O., Weber, S., Jacob, V., Canete, T., Albinet, A., Charron, A., Riffault, V., Perdrix, E., Waked, A., Golly, B., Salameh, D., Chevrier, F., Oliveira, D. M., Besombes, J.-L., Martins, J. M. F., Bonnaire, N., Conil, S., Guillaud, G., Mesbah, B., Rocq, B., Robic, P.-Y., Hulin, A., Le Meur, S., Descheemaecker, M., Chretien, E., Marchand, N., and Uzu, G.: Arabitol, mannitol, and glucose as tracers of primary biogenic organic aerosol: the influence of environmental factors on ambient air concentrations and spatial distribution over France, Atmos. Chem. Phys., 19, 11013–11030, https://doi.org/10.5194/acp-19-11013-2019, 2019a.

Samaké, A., Jaffrezo, J.-L., Favez, O., Weber, S., Jacob, V., Albinet, A., Riffault, V., Perdrix, E., Waked, A., Golly, B., Salameh, D., Chevrier, F., Oliveira, D. M., Bonnaire, N., Besombes, J.-L., Martins, J. M. F., Conil, S., Guillaud, G., Mesbah, B., Rocq, B., Robic, P.-Y., Hulin, A., Le Meur, S., Descheemaecker, M., Chretien, E., Marchand, N., and Uzu, G.: Polyols and glucose particulate species as tracers of primary biogenic organic

aerosols at 28 French sites, Atmos. Chem. Phys., 19, 3357–3374, https://doi.org/10.5194/acp-19-3357-2019, 2019b.

Schauer, J. J. and Cass, G. R.: Source Apportionment of Wintertime Gas-Phase and Particle-Phase Air Pollutants Using Organic Compounds as Tracers, Environ. Sci. Technol., 34, 1821–1832, https://doi.org/10.1021/es981312t, 2000.

Schneider, W. F., Li, J., and Hass, K. C.: Combined Computational and Experimental Investigation of SO$_x$ Adsorption on MgO, J. Phys. Chem. B, 105, 6972–6979, https://doi.org/10.1021/jp010747r, 2001.

Seinfeld, J. H. and Pankow, J. F.: Organic Atmospheric Particulate Material, Annu. Rev. Phys. Chem., 54, 121–140, https://doi.org/10.1146/annurev.physchem.54.011002.103756, 2003.

Shiraiwa, M., Ueda, K., Pozzer, A., Lammel, G., Kampf, C. J., Fushimi, A., Enami, S., Arangio, A. M., Fröhlich-Nowoisky, J., Fujitani, Y., Furuyama, A., Lakey, P. S. J., Lelieveld, J., Lucas, K., Morino, Y., Pöschl, U., Takahama, S., Takami, A., Tong, H., Weber, B., Yoshino, A., and Sato, K.: Aerosol Health Effects from Molecular to Global Scales, Environ. Sci. Technol., 51, 13545–13567, https://doi.org/10.1021/acs.est.7b04417, 2017.

Shrivastava, M. K., Subramanian, R., Rogge, W. F., and Robinson, A. L.: Sources of organic aerosol: Positive matrix factorization of molecular marker data and comparison of results from different source apportionment models, Atmos. Environ., 41, 9353–9369, https://doi.org/10.1016/j.atmosenv.2007.09.016, 2007.

Srivastava, D., Favez, O., Perraudin, E., Villenave, E., and Albinet, A.: Comparison of Measurement-Based Methodologies to Apportion Secondary Organic Carbon (SOC) in PM$_{2.5}$: A Review of Recent Studies, Atmosphere, 9, 452, https://doi.org/10.3390/atmos9110452, 2018a.

Srivastava, D., Tomaz, S., Favez, O., Lanzafame, G. M., Golly, B., Besombes, J.-L., Alleman, L. Y., Jaffrezo, J.-L., Jacob, V., Perraudin, E., Villenave, E., and Albinet, A.: Speciation of organic fraction does matter for source apportionment. Part 1: A one-year campaign in Grenoble (France), Sci. Total Environ., 624, 1598–1611, https://doi.org/10.1016/j.scitotenv.2017.12.135, 2018b.

Surratt, J. D., Chan, A. W. H., Eddingsaas, N. C., Chan, M., Loza, C. L., Kwan, A. J., Hersey, S. P., Flagan, R. C., Wennberg, P. O., and Seinfeld, J. H.: Reactive intermediates revealed in secondary organic aerosol formation from isoprene, Proceedings of the National Academy of Sciences, 107, 6640–6645, https://doi.org/10.1073/pnas.0911114107, 2010.

Szmigielski, R., Surratt, J. D., Gómez-González, Y., Van der Veken, P., Kourtchev, I., Vermeylen, R., Blockhuys, F., Jaoui, M., Kleindienst, T. E., Lewandowski, M., Offenberg, J. H., Edney, E. O., Seinfeld, J. H., Maenhaut, W., and Claeys, M.: 3-methyl-1,2,3-butanetricarboxylic acid: An atmospheric tracer for terpene secondary organic aerosol, Geophys. Res. Lett., 34, L24811, https://doi.org/10.1029/2007GL031338, 2007.

Ullerstam, M., Vogt, R., Langer, S., and Ljungström, E.: The kinetics and mechanism of SO$_2$ oxidation by O$_3$ on mineral dust, Phys. Chem. Chem. Phys., 4, 4694–4699, https://doi.org/10.1039/B203529B, 2002.

Ullerstam, M., Johnson, M. S., Vogt, R., and Ljungström, E.: DRIFTS and Knudsen cell study of the heterogeneous reactivity of SO$_2$ and NO$_2$ on mineral dust, Atmos. Chem. Phys., 3, 2043–2051, https://doi.org/10.5194/acp-3-2043-2003, 2003.

Usher, C. R., Al-Hosney, H., Carlos-Cuellar, S., and Grassian, V. H.: A laboratory study of the heterogeneous uptake and oxidation of sulfur dioxide on mineral dust particles: Uptake of Sulfur Dioxide on Dust, J. Geophys. Res., 107, ACH 16-1–ACH 16-9, https://doi.org/10.1029/2002JD002051, 2002.

van Drooge, B. L. and Grimalt, J. O.: Particle size-resolved source apportionment of primary and secondary organic tracer compounds at urban and rural locations in Spain, Atmos. Chem. Phys., 15, 7735–7752, https://doi.org/10.5194/acp-15-7735-2015, 2015.

Verma, S. K., Kawamura, K., Chen, J., and Fu, P.: Thirteen years of observations on primary sugars and sugar alcohols over remote Chichijima Island in the western North Pacific, Atmos. Chem. Phys., 18, 81–101, https://doi.org/10.5194/acp-18-81-2018, 2018.

Vlachou, A., Tobler, A., Lamkaddam, H., Canonaco, F., Daellenbach, K. R., Jaffrezo, J.-L., Minguillón, M. C., Maasikmets, M., Teinemaa, E., Baltensperger, U., El Haddad, I., and Prévôt, A. S. H.: Development of a versatile source apportionment analysis based on positive matrix factorization: a case study of the seasonal variation of organic aerosol sources in Estonia, Atmos. Chem. Phys., 19, 7279–7295, https://doi.org/10.5194/acp-19-7279-2019, 2019.

Waked, A., Favez, O., Alleman, L. Y., Piot, C., Petit, J.-E., Delaunay, T., Verlinden, E., Golly, B., Besombes, J.-L., Jaffrezo, J.-L., and Leoz-Garziandia, E.: Source apportionment of PM$_{10}$ in a north-western Europe regional urban background site (Lens, France) using positive matrix factorization and including primary biogenic emissions, Atmos. Chem. Phys., 14, 3325–3346, https://doi.org/10.5194/acp-14-3325-2014, 2014.

Wang, Q., He, X., Huang, X. H. H., Griffith, S. M., Feng, Y., Zhang, T., Zhang, Q., Wu, D., and Yu, J. Z.: Impact of Secondary Organic Aerosol Tracers on Tracer-Based Source Apportionment of Organic Carbon and PM$_{2.5}$: A Case Study in the Pearl River Delta, China, ACS Earth Space Chem., 1, 562–571, https://doi.org/10.1021/acsearthspacechem.7b00088, 2017a.

Wang, Q., Jiang, N., Yin, S., Li, X., Yu, F., Guo, Y., and Zhang, R.: Carbonaceous species in PM$_{2.5}$ and PM$_{10}$ in urban area of Zhengzhou in China: Seasonal variations and source apportionment, Atmos. Res., 191, 1–11, https://doi.org/10.1016/j.atmosres.2017.02.003, 2017b.

Wang, Y., Hopke, P. K., Xia, X., Rattigan, O. V., Chalupa, D. C., and Utell, M. J.: Source apportionment of airborne particulate matter using inorganic and organic species as tracers, Atmos. Environ., 55, 525–532, https://doi.org/10.1016/j.atmosenv.2012.03.073, 2012.

Warneck, P.: Chemistry of the natural atmosphere, 2nd ed., Academic Press, San Diego, 2000.

Weber, S., Salameh, D., Albinet, A., Alleman, L. Y., Waked, A., Besombes, J.-L., Jacob, V., Guillaud, G., Meshbah, B., Rocq, B., Hulin, A., Dominik-Sègue, M., Chrétien, E., Jaffrezo, J.-L., and Favez, O.: Comparison of PM$_{10}$ Sources Profiles at 15 French Sites Using a Harmonized Constrained Positive Matrix Factorization Approach, Atmosphere, 10, 310, https://doi.org/10.3390/atmos10060310, 2019.

Willers, S. M., Eriksson, C., Gidhagen, L., Nilsson, M. E., Pershagen, G., and Bellander, T.: Fine and coarse particulate air pollution in relation to respiratory health in Sweden, Eur. Respir. J., 42, 924–934, https://doi.org/10.1183/09031936.00088212, 2013.

Wilson, R. and Spengler, J. D. (Eds.): Particles in our air: concentrations and health effects, Harvard School of Public Health; distributed by Harvard University Press, Cambridge, MA, 1996.

Yan, Y., He, Q., Guo, L., Li, H., Zhang, H., Shao, M., and Wang, Y.: Source apportionment and toxicity of atmospheric polycyclic aromatic hydrocarbons by PMF: Quantifying the influence of coal usage in Taiyuan, China, Atmos. Res., 193, 50–59, https://doi.org/10.1016/j.atmosres.2017.04.001, 2017.

Yang, F., Kawamura, K., Chen, J., Ho, K., Lee, S., Gao, Y., Cui, L., Wang, T., and Fu, P.: Anthropogenic and biogenic organic compounds in summertime fine aerosols (PM$_{2.5}$) in Beijing, China, Atmos. Environ., 124, 166–175, https://doi.org/10.1016/j.atmosenv.2015.08.095, 2016.

Yang, X., Feng, L., Zhang, Y., Hu, H., Shi, Y., Liang, S., Zhao, T., Fu, Y., Duan, J., and Sun, Z.: Cytotoxicity induced by fine particulate matter (PM$_{2.5}$) via mitochondria-mediated apoptosis pathway in human cardiomyocytes, Ecotox. Environ. Safe., 161, 198–207, https://doi.org/10.1016/j.ecoenv.2018.05.092, 2018.

Yuan, Z., Lau, A., Zhang, H., Yu, J., Louie, P., and Fung, J.: Identification and spatiotemporal variations of dominant PM$_{10}$ sources over Hong Kong, Atmos. Environ., 40, 1803–1815, https://doi.org/10.1016/j.atmosenv.2005.11.030, 2006.

Zhang, Y., Tang, L., Sun, Y., Favez, O., Canonaco, F., Albinet, A., Couvidat, F., Liu, D., Jayne, J. T., Wang, Z., Croteau, P. L., Canagaratna, M. R., Zhou, H., Prévôt, A. S. H., and Worsnop, D. R.: Limited formation of isoprene epoxydiols-derived secondary organic aerosol under NO$_x$-rich environments in Eastern China: Limited Formation of IEPOX-SOA, Geophys. Res. Lett., 44, 2035–2043, https://doi.org/10.1002/2016GL072368, 2017.

Zhang, Y. Y., Müller, L., Winterhalter, R., Moortgat, G. K., Hoffmann, T., and Pöschl, U.: Seasonal cycle and temperature dependence of pinene oxidation products, dicarboxylic acids and nitrophenols in fine and coarse air particulate matter, Atmos. Chem. Phys., 10, 7859–7873, https://doi.org/10.5194/acp-10-7859-2010, 2010.

Zheng, J., Tan, M., Shibata, Y., Tanaka, A., Li, Y., Zhang, G., Zhang, Y., and Shan, Z.: Characteristics of lead isotope ratios and elemental concentrations in PM$_{10}$ fraction of airborne particulate matter in Shanghai after the phase-out of leaded gasoline, Atmos. Environ., 38, 1191–1200, https://doi.org/10.1016/j.atmosenv.2003.11.004, 2004.

Zhu, Y., Huang, L., Li, J., Ying, Q., Zhang, H., Liu, X., Liao, H., Li, N., Liu, Z., Mao, Y., Fang, H., and Hu, J.: Sources of particulate matter in China: Insights from source apportionment studies published in 1987–2017, Environ. Int., 115, 343–357, https://doi.org/10.1016/j.envint.2018.03.037, 2018.